

 Open access • Posted Content • DOI:10.1101/2021.05.13.443778

## **STING mediates immune responses in the closest living relatives of animals**

— [Source link](#) 

[Arielle Woznica](#), [Ashwani Kumar](#), [Carolyn R. Sturge](#), [Chao Xing](#) ...+2 more authors

**Institutions:** [University of Texas Southwestern Medical Center](#), [Howard Hughes Medical Institute](#)

**Published on:** 30 Sep 2021 - [bioRxiv](#) (Cold Spring Harbor Laboratory)

**Topics:** [Innate immune system](#)

Related papers:

- [STING mediates immune responses in the closest living relatives of animals.](#)
- [STING mediates immune responses in a unicellular choanoflagellate](#)
- [Analysis of Drosophila STING Reveals an Evolutionarily Conserved Antimicrobial Function](#)
- [The STING ligand 2'3'-cGAMP induces an NF-κB-dependent anti-bacterial innate immune response in the starlet sea anemone Nematostella vectensis](#)
- [Innate immunity of plants, animals, and humans](#)

Share this paper:    

View more about this paper here: <https://typeset.io/papers/sting-mediates-immune-responses-in-the-closest-living-1dbdseda9>

# 1 **STING mediates immune responses in the closest living relatives of animals**

2  
3 Arielle Woznica<sup>1\*</sup>, Ashwani Kumar<sup>2</sup>, Carolyn R. Sturge<sup>1</sup>, Chao Xing<sup>2</sup>, Nicole King<sup>3</sup>, Julie  
4 K. Pfeiffer<sup>1\*</sup>

5  
6 <sup>1</sup> Department of Microbiology, University of Texas Southwestern Medical Center, Dallas  
7 TX 75390, USA

8 <sup>2</sup> McDermott Center Bioinformatics Lab, University of Texas Southwestern Medical  
9 Center, Dallas TX, USA

10 <sup>3</sup> Howard Hughes Medical Institute, and Department of Molecular and Cell Biology,  
11 University of California, Berkeley, Berkeley, CA 94720, USA.

12  
13 \*Correspondence: [Arielle.Woznica@UTSouthwestern.edu](mailto:Arielle.Woznica@UTSouthwestern.edu) and  
14 [Julie.Pfeiffer@UTSouthwestern.edu](mailto:Julie.Pfeiffer@UTSouthwestern.edu)

## 15 16 17 **Abstract**

18  
19  
20 Animals have evolved unique repertoires of innate immune genes and pathways that  
21 provide their first line of defense against pathogens. To reconstruct the ancestry of  
22 animal innate immunity, we have developed the choanoflagellate *Monosiga brevicollis*,  
23 one of the closest living relatives of animals, as a model for studying mechanisms  
24 underlying pathogen recognition and immune response. We found that *M. brevicollis* is  
25 killed by exposure to *Pseudomonas aeruginosa* bacteria. Moreover, *M. brevicollis*  
26 expresses STING, which, in animals, activates innate immune pathways in response to  
27 cyclic dinucleotides during pathogen sensing. *M. brevicollis* STING increases the  
28 susceptibility of *M. brevicollis* to *P. aeruginosa*-induced cell death and is required for  
29 responding to the cyclic dinucleotide 2'3' cGAMP. Furthermore, similar to animals,  
30 autophagic signaling in *M. brevicollis* is induced by 2'3' cGAMP in a STING-dependent  
31 manner. This study provides evidence for a pre-animal role for STING in antibacterial  
32 immunity and establishes *M. brevicollis* as a model system for the study of immune  
33 responses.

34  
35  
36  
37  
38  
39  
40

## 41 Introduction

42

43 Innate immunity is the first line of defense against pathogens for all animals, in  
44 which it is crucial for distinguishing between self and non-self, recognizing and  
45 responding to pathogens, and repairing cellular damage. Some mechanisms of animal  
46 immunity have likely been present since the last common eukaryotic ancestor, including  
47 RNAi, production of antimicrobial peptides, and the production of nitric oxide<sup>1,2</sup>.  
48 However, many gene families that play critical roles in animal innate immune responses  
49 are unique to animals<sup>3</sup>.

50 Comparing animals with their closest relatives, the choanoflagellates, can  
51 provide unique insights into the ancestry of animal immunity and reveal other key  
52 features of the first animal, the ‘Urmetazoan’<sup>4–6</sup>. Choanoflagellates are microbial  
53 eukaryotes that live in diverse aquatic environments and survive by capturing and  
54 phagocytosing environmental bacteria<sup>7</sup> using their “collar complex,” an apical flagellum  
55 surrounded by actin-filled microvilli (Figure 1A)<sup>7,8</sup>. Several innate immune pathway  
56 genes once considered to be animal-specific are present in choanoflagellates, including  
57 cGAS and STING, both of which are crucial for innate responses to cytosolic DNA in  
58 animals (Figure 1- Supplement 1)<sup>3,9,10</sup>. Although the phylogenetic distribution of these  
59 gene families reveals that they first evolved before animal origins, their functions in  
60 choanoflagellates and their contributions to the early evolution of animal innate  
61 immunity are unknown.

62 STING (stimulator of interferon genes) is a signaling protein that activates innate  
63 immune responses to cytosolic DNA during bacterial or viral infection<sup>11,12</sup>. Although  
64 STING homologs are conserved in diverse invertebrate and vertebrate animals  
65 (reviewed in Margolis et al. 2017)<sup>9,13,14</sup>, mechanisms of STING activation are best  
66 understood in mammals. In mammals, STING is activated by binding 2’3’ cGAMP, an  
67 endogenous cyclic dinucleotide produced by the sensor cGAS (cyclic GMP-AMP  
68 synthase) upon detecting cytosolic DNA<sup>15–20</sup>. In addition, cyclic dinucleotides produced  
69 by bacteria can also activate STING<sup>17,21</sup>. Importantly, STING domain-containing  
70 systems are present in bacteria where they may contribute to anti-phage defense<sup>22,23</sup>,  
71 raising the possibility that eukaryotic STING-like proteins were acquired from lateral  
72 gene transfer<sup>24</sup>. Comparative genomics suggests that STING domains arose at least  
73 three independent times in eukaryotes, including once in the stem lineage leading to  
74 Choanozoa, the clade containing animals and choanoflagellates<sup>24</sup>.

75 Choanoflagellates have already served as powerful models for studying the  
76 origin of animal multicellularity and cell differentiation<sup>10,25–30</sup> and are ideally positioned to  
77 yield insights into the evolution of animal immune pathways. Therefore, we sought to  
78 establish the choanoflagellate *Monosiga brevicollis* as a model for studying pathogen  
79 recognition and immune responses. Here, we report that *Pseudomonas aeruginosa*  
80 bacteria are pathogenic for *M. brevicollis*. Through our study of interactions between *P.*

81 *aeruginosa* and *M. brevicollis*, we determined that STING functions in the  
82 choanoflagellate antibacterial response. In addition, we demonstrate that STING is  
83 necessary for mediating responses to the STING agonist 2'3' cGAMP *in vivo*, and that  
84 2'3' cGAMP induces STING-dependent autophagic signaling. Our results demonstrate  
85 that key features of STING-mediated immune responses are conserved in *M.*  
86 *brevicollis*, thereby expanding our understanding of the pre-metazoan ancestry of  
87 STING signaling.

88

## 89 **Results**

90

### 91 ***P. aeruginosa* has pathogenic effects on *M. brevicollis***

92

93 One impediment to studying immune responses in choanoflagellates has been  
94 the lack of known choanoflagellate pathogens. While bacteria are obligate prey and can  
95 regulate mating, multicellular development, and cell contractility in choanoflagellates, to  
96 our knowledge no bacteria with pathogenic effects have been described<sup>25,28,29,31–33</sup>. For  
97 this study, we focused on the choanoflagellate *Monosiga brevicollis*, which has a  
98 sequenced genome<sup>4</sup> and grows robustly under laboratory conditions in co-culture with  
99 *Flavobacterium* prey bacteria<sup>5</sup>. To identify potential pathogens of choanoflagellates, we  
100 screened select bacteria – including environmental isolates and known animal  
101 pathogens and commensals (Table 1) – to test whether any of these induced *M.*  
102 *brevicollis* behavioral changes or reduced cell survival.

103 After co-culturing *M. brevicollis* with bacteria for 24 hours, only the  
104 gammaproteobacterium *Pseudomonas aeruginosa*, a ubiquitous environmental  
105 bacterium and opportunistic pathogen of diverse eukaryotes<sup>34–37</sup>, altered the behavior  
106 and growth dynamics of *M. brevicollis*. Under standard laboratory conditions, *M.*  
107 *brevicollis* is a highly motile flagellate and swims up in the water column (Video 1,  
108 Supplementary file 1). However, after 12-14 hours in the presence of *P. aeruginosa*  
109 strains PAO1 and PA14, a large proportion of *M. brevicollis* cells settled to the bottom of  
110 the culture dish (Video 1, Supplementary file 1). Immunofluorescence staining revealed  
111 that *M. brevicollis* cells exposed to *P. aeruginosa* had truncated flagella compared to  
112 cells exposed to *E. coli* or other bacteria that did not induce cell settling (Figure 1B). To  
113 determine the effects of *P. aeruginosa* on cell viability, we added *P. aeruginosa* strain  
114 PAO1 or control gammaproteobacteria to *M. brevicollis* and monitored cell density over  
115 the course of 72 hours (Figure 1C). While *M. brevicollis* continued to proliferate in the  
116 presence of control gammaproteobacteria, exposure to *P. aeruginosa* PAO1 resulted in  
117 cell death.

118 Choanoflagellates prey upon bacteria and ingest them through phagocytosis<sup>7,8</sup>.  
119 However, many bacterial pathogens, including *P. aeruginosa*, have evolved strategies  
120 to prevent or resist phagocytosis by eukaryotic cells<sup>38,39</sup>. Therefore, we examined

121 whether phagocytosis of *P. aeruginosa* is required to induce cell death. To track  
122 phagocytosis, we added GFP-expressing *E. coli* DH5 $\alpha$  (Figure 1D) or *P. aeruginosa*  
123 PAO1 (Figure 1E) to *M. brevicollis* and monitored the cultures by live imaging. After one  
124 hour, while 92% of *M. brevicollis* cells incubated with *E. coli*-GFP had GFP+ food  
125 vacuoles, only 3% of cells incubated with PAO1-GFP had GFP+ food vacuoles (Figure  
126 1F). *M. brevicollis* also robustly phagocytosed GFP-expressing *V. parahaemolyticus*  
127 and *C. jejuni* (Figure 1F).

128 Next, to determine if *P. aeruginosa* broadly disrupts *M. brevicollis* phagocytosis,  
129 which could induce cell death through starvation, we incubated *M. brevicollis* with GFP-  
130 expressing PAO1 or GFP-expressing *E. coli* for one hour, and then added 0.2  $\mu$ m  
131 fluorescent beads for an additional 30 minutes as an independent measure of  
132 phagocytic activity. The fraction of *M. brevicollis* cells with internalized 0.2  $\mu$ m beads  
133 was similar in cultures incubated with *E. coli* DH5 $\alpha$  and PAO1 (Figure 1G). Moreover,  
134 exposure to *P. aeruginosa* did not inhibit phagocytic uptake of *E. coli* (Figure 1H). These  
135 results suggest that exposure to *P. aeruginosa* does not broadly inhibit phagocytosis.

136 The above results suggested that the pathogenic effects of *P. aeruginosa* are  
137 induced by factors secreted by extracellular bacteria. In addition, diverse secreted  
138 bacterial molecules have been previously shown to influence choanoflagellate cell  
139 biology<sup>25,28,31</sup>. Therefore, we next investigated the effects of secreted *P. aeruginosa*  
140 molecules on *M. brevicollis* viability. Exposure of *M. brevicollis* to conditioned medium  
141 from *P. aeruginosa* PAO1 or diverse non-pathogenic gammaproteobacteria revealed  
142 that PAO1 conditioned medium is sufficient to restrict growth and induce cell death  
143 (Figure 1I). Similar to live bacteria, exposure to *P. aeruginosa* conditioned medium led  
144 to reduced motility and truncated flagella in *M. brevicollis* after approximately 8-10  
145 hours.

146 Because numerous *P. aeruginosa* secreted virulence factors have been  
147 characterized<sup>34,40</sup>, we screened a battery of isogenic PAO1 strains with deletions in  
148 known virulence genes to determine if any of these factors contribute to the pathogenic  
149 effects on *M. brevicollis* (Table 2). All strains tested induced similar levels of *M.*  
150 *brevicollis* cell death as the parental PAO1 strain, suggesting that none of the deleted  
151 virulence genes alone are essential for inducing cytotoxicity in *M. brevicollis*. The  
152 bioactivity in the conditioned media was also found to be heat, protease, and nuclease  
153 resistant, indicating that the virulence factors are unlikely to be proteins or nucleic acids  
154 (Table 3). In addition, we found that subjecting the conditioned media to methanol  
155 extraction followed by liquid chromatography-mass spectrometry resulted in specific  
156 fractions that recapitulated the bioactivity of the conditioned media. Although further  
157 detailed chemical analysis is required to determine the molecular nature of these  
158 factors, these data indicate that secreted *P. aeruginosa* small molecules are sufficient  
159 for inducing cell death in *M. brevicollis*.

160 Finally, we investigated whether transient exposure to *P. aeruginosa* is sufficient  
161 to induce cell death in *M. brevicollis* (Figure 1J). Because choanoflagellates likely  
162 experience fluctuations in the chemical composition of aquatic microenvironments on  
163 various timescales, we exposed stationary-phase *M. brevicollis* to *P. aeruginosa*  
164 conditioned media for increasing durations, and then assessed survival relative to  
165 *Flavobacterium*-treated controls after 24 hours. While *M. brevicollis* cell death was not  
166 observed after treatment with *P. aeruginosa* conditioned media for 4 hours or less,  
167 exposures lasting for 6 hours or longer reduced *M. brevicollis* survival (Figure 1J).  
168 These results suggest that cell death pathways are not induced immediately in  
169 response *P. aeruginosa* virulence factors, but are activated after longer exposures to *P.*  
170 *aeruginosa*.

171

### 172 **Upregulation of *M. brevicollis* STING in response to *P. aeruginosa***

173

174 To identify potential genetic pathways activated by *M. brevicollis* in response to  
175 pathogenic bacteria, we performed RNA-seq on *M. brevicollis* exposed to conditioned  
176 medium from either *P. aeruginosa* or *Flavobacterium sp.*, the non-pathogenic bacterial  
177 strain used as a food source (Table 1). We found that 674 genes were up-regulated  
178 and 232 genes were downregulated two-fold or greater ( $FDR \leq 10^{-4}$ ) upon *P. aeruginosa*  
179 exposure compared to cells exposed to *Flavobacterium* (Figure 2A). The up-regulated  
180 genes were enriched in biological processes including response to stress, endocytosis,  
181 microtubule-based movement, mitochondrial fission, and carbohydrate metabolism.  
182 Genes down-regulated in response to *P. aeruginosa* were enriched in biological  
183 processes including RNA modification and metabolism (Figure 2 - figure supplement  
184 1A). We also found that the transcription of several genes encoding proteins that  
185 function in animal antibacterial innate immunity was upregulated in response to *P.*  
186 *aeruginosa*, including C-type lectin, glutathione peroxidase, and STING (Figure 2A,B).  
187 Using an antibody we raised against the C-terminal portion of *M. brevicollis* STING  
188 (Figure 2 - figure supplement 1C) we found that STING protein levels are also elevated  
189 in response to *P. aeruginosa* (Figure 2C). Given the importance of STING in animal  
190 immunity and its upregulation in response to *P. aeruginosa*, we pursued its functional  
191 relevance in the *M. brevicollis* pathogen response.

192

### 193 **The cyclic dinucleotide 2'3' cGAMP induces elevated expression of STING in *M.*** 194 ***brevicollis***

195

196 The predicted domain architecture of *M. brevicollis* STING consists of four  
197 transmembrane domains followed by a cytosolic STING domain (Fig. 3A, Figure 2 -  
198 figure supplement 1D), and likely matches the structure of the ancestral animal STING  
199 protein. Vertebrate STING proteins contain a C-terminal tail (CTT; Fig. 3A, Figure 2 -

200 figure supplement 1D) that is required for the induction of interferons<sup>41-43</sup>, and for the  
201 activation of other downstream responses, including NFkB<sup>44</sup> and autophagy<sup>45-47</sup>  
202 pathways. Both the STING CTT and interferons evolved in vertebrates, and it is  
203 currently unclear how choanoflagellate and invertebrate STING proteins mediate  
204 downstream immune responses<sup>13,48</sup>. However, the conservation of putative cyclic  
205 dinucleotide-binding residues in *M. brevicollis* STING (Fig. 3B) led us to hypothesize  
206 that STING signaling may be induced by cyclic dinucleotides. In addition, because *M.*  
207 *brevicollis* has a cGAS-like enzyme (Figure 1- Supplement 1A), it is possible that *M.*  
208 *brevicollis* produces an endogenous cyclic dinucleotide similar to mammalian 2'3'  
209 cGAMP<sup>9,12,49</sup>.

210 To identify potential STING inducers<sup>49,50</sup>, we treated *M. brevicollis* with purified  
211 cyclic dinucleotides, including mammalian cGAMP (2'3' cGAMP) and bacterial cyclic  
212 dinucleotides (3'3' c-di-GMP, 3'3' c-di-AMP, 3'3' cGAMP). We first performed dose-  
213 response curves to determine if the different cyclic dinucleotides affect the viability of *M.*  
214 *brevicollis* (Fig. 3C). Interestingly, we found that exposure to 2'3' cGAMP induced cell  
215 death in a dose-dependent manner. In contrast, exposure to 3'3' cGAMP, c-di-GMP,  
216 and c-di-AMP did not alter *M. brevicollis* survival. Transcriptional profiling of *M.*  
217 *brevicollis* revealed a robust transcriptional response to 2'3' cGAMP after three hours  
218 (Figure 3 - figure supplement 1A). Moreover, transcriptional profiling of *M. brevicollis*  
219 exposed to 2'3' cGAMP or 3'3' cGAMP for three hours revealed that *STING* mRNA  
220 levels increase in response to 2'3' cGAMP, but remain unchanged in response to 3'3'  
221 cGAMP (Figure 3 - figure supplement 1A-C). Therefore, we next treated *M. brevicollis*  
222 with the cyclic dinucleotides for five hours, and measured STING protein levels by  
223 immunoblot (Fig. 3D). Treatment with 2'3' cGAMP, but not the bacterially-produced  
224 cyclic dinucleotides, led to elevated levels of STING protein compared to unstimulated  
225 cells. A time course of 2'3' cGAMP treatment revealed that STING protein levels  
226 increase as early as three hours after exposure to the cyclic dinucleotide and remain  
227 elevated for at least 7 hours, approximately one cell cycle (Fig. 3E). While we also  
228 observed sustained upregulation of STING in the presence of *P. aeruginosa*, this is  
229 markedly different from what has been described in mammals, wherein STING  
230 activation results in its translocation to lysosomes and degradation<sup>47</sup>. In addition,  
231 immunostaining for STING in fixed *M. brevicollis* revealed that the number and intensity  
232 of STING puncta increases after exposure to 2'3' cGAMP (Figure 3 - figure supplement  
233 1E,F), although the localization of STING was difficult to assess by immunostaining due  
234 to a lack of available subcellular markers. These data suggest that *M. brevicollis* STING  
235 responds to 2'3' cGAMP, and that this cyclic dinucleotide can be used to further  
236 characterize the role of STING in *M. brevicollis*.

237

238 **Transfection reveals that STING localizes to the *M. brevicollis* endoplasmic**  
239 **reticulum**

240

241 A key barrier to investigating gene function in *M. brevicollis* has been the  
242 absence of transfection and reverse genetics. We found that the transfection protocol  
243 recently developed for the choanoflagellate *Salpingoeca rosetta*<sup>50</sup> was not effective in  
244 *M. brevicollis*, but by implementing a number of alterations to optimize reagents and  
245 conditions (see Methods) we were able to achieve both reproducible transfection and  
246 establishment of stably transformed cell lines in *M. brevicollis*.

247 To investigate the subcellular localization of STING, we established a robust  
248 transfection protocol for *M. brevicollis* that would allow the expression of fluorescently-  
249 labeled STING along with fluorescent subcellular markers for different organelles.  
250 We observed that STING-mTFP protein localized to tubule-like structures around the  
251 nucleus (Figure 5A) similar to what was observed by immunostaining with an antibody  
252 to STING (Figure 3 - figure supplement 1E,F). We then co-transfected STING-mTFP  
253 alongside fluorescent reporters marking the endoplasmic reticulum (ER) or mitochondria  
254 (Figure 5B,C) and performed live-cell imaging. STING-mTFP co-localized with a  
255 fluorescent marker highlighting the ER (Figure 5B). Thus, as in mammalian cells<sup>15,51</sup>,  
256 STING localizes to regions of the ER in *M. brevicollis*.

257

### 258 **Genetic disruption of STING reveals its role in responding to 2'3' cGAMP and *P.*** 259 ***aeruginosa***

260

261 Disrupting the *STING* locus using CRISPR/Cas9-mediated genome editing  
262 (Figure 5A) enabled us to investigate the function of STING. To overcome low gene  
263 editing efficiencies in *M. brevicollis*, we based our gene editing strategy on a protocol  
264 recently developed for *S. rosetta* that simultaneously edits a gene of interest and  
265 confers cycloheximide resistance<sup>52</sup>. By selecting for cycloheximide resistance and then  
266 performing clonal isolation, we were able to isolate a clonal cell line that has a deletion  
267 within the *STING* locus that introduces premature stop codons (Figure 5 - figure  
268 supplement 1A). We were unable to detect STING protein in *STING*<sup>-</sup> cells by  
269 immunoblot (Figure 5B). Wild type and *STING*<sup>-</sup> cells have similar growth kinetics (Figure  
270 5 - figure supplement 1B), suggesting that STING is not required for cell viability under  
271 standard laboratory conditions. In addition, overexpression of STING-mTFP did not  
272 affect *M. brevicollis* viability.

273 To investigate the connection between 2'3' cGAMP and STING signaling in *M.*  
274 *brevicollis*, we exposed *STING*<sup>-</sup> cells to increasing concentrations of 2'3' cGAMP. In  
275 contrast to wild type *M. brevicollis*, *STING*<sup>-</sup> cells are resistant to 2'3' cGAMP-induced  
276 cell death (Figure 5C). The 2'3' cGAMP resistance phenotype could be partially  
277 reversed by stably expressing STING within the *STING*<sup>-</sup> mutant background (Figure  
278 5D). In addition, *STING*<sup>-</sup> cells fail to induce a strong transcriptional response to 2'3'  
279 cGAMP compared to wild type cells (Figure 5E, Figure 3 - figure supplement 1A, Figure



280 5 - figure supplement 1C,D). While 371 genes are differentially expressed in wild type  
281 cells after exposure to 2'3' cGAMP for three hours, only 28 genes are differentially  
282 expressed in *STING*<sup>-</sup> cells (FC ≥3; FDR ≤10<sup>-4</sup>). Thus, 2'3' cGAMP induces a STING-  
283 dependent transcriptional response in *M. brevicollis*.

284 Interestingly, of the 22 choanoflagellate species with sequenced  
285 transcriptomes<sup>3,29</sup>, only *M. brevicollis* and *Salpingoeca macrocollata*, express homologs  
286 of both STING and cGAS (Figure 1- Supplement 1A, Figure 5F, Figure 5 - figure  
287 supplement 1E). Therefore, we were curious whether other choanoflagellate species  
288 are able to respond to 2'3' cGAMP in the absence of a putative STING protein. We  
289 exposed four other choanoflagellate species (*Salpingoeca infusionum*, *S. macrocollata*,  
290 *S. rosetta*, and *Salpingoeca punica*) to increasing 2'3' cGAMP concentrations, and  
291 quantified survival after 24 hours (Figure 5G). Of these additional species, only *S.*  
292 *macrocollata* had impaired survival in the presence of 2'3' cGAMP. Thus, it is possible  
293 that STING also responds to 2'3' cGAMP in *S. macrocollata*.

294 We next asked whether *STING*<sup>-</sup> cells have altered responses to other immune  
295 agonists. Although *M. brevicollis* is continuously co-cultured with feeding bacteria, we  
296 observed that treatment with high concentrations of *E. coli* lipopolysaccharides induces  
297 cell death (Figure 5H). As LPS is not known to activate STING signaling, we treated wild  
298 type and *STING*<sup>-</sup> cells with LPS to probe the specificity of STING-mediated immune  
299 responses in *M. brevicollis*. The survival responses of wild type and *STING*<sup>-</sup> cells to  
300 LPS were indistinguishable (Figure 5H), suggesting that there are separable pathways  
301 for responding to 2'3' cGAMP and LPS. We also examined the survival of *STING*<sup>-</sup> cells  
302 exposed to *P. aeruginosa* conditioned medium (Figure 5I,J). In growth curve  
303 experiments, *P. aeruginosa* hindered the growth rate and stationary phase cell density  
304 of *STING*<sup>-</sup> cells compared to *Flavobacterium* (Figure 5I,J). However, *STING*<sup>-</sup> cells were  
305 still able to divide in the presence of *P. aeruginosa*, whereas wild type cell growth was  
306 completely restricted (Figure 5I,J). These results indicate that wild type cells are more  
307 susceptible to *P. aeruginosa* than *STING*<sup>-</sup> cells, although it is unclear how STING  
308 contributes to *P. aeruginosa*-induced growth restriction and cell death.

309  
310

## 311 **2'3' cGAMP-induces autophagic signaling via STING**

312

313 One downstream consequence of STING signaling in animals is the initiation of  
314 autophagy<sup>21,45,46,49,53</sup>. Based on viral infection studies in *D. melanogaster*<sup>53</sup> and  
315 experiments expressing invertebrate STING in mammalian cells<sup>45</sup>, it has been  
316 proposed that the induction of autophagy may be an interferon-independent ancestral  
317 function of STING. Although *M. brevicollis* lacks many effectors required for immune  
318 responses downstream of STING in animals (including TBK1 and NF-κB; Figure S1A),

319 autophagy machinery is well conserved in *M. brevicollis*. Therefore, we asked if one  
320 outcome of 2'3' cGAMP exposure in *M. brevicollis* is the induction of autophagy.

321 The evolutionarily conserved protein Atg8/LC3 is a ubiquitin-like protein that can  
322 be used to monitor autophagy<sup>54,55</sup>. During autophagosome formation, unmodified Atg8,  
323 called Atg8-I, is conjugated to phosphatidylethanolamine. Lipidated Atg8, called Atg8-II,  
324 remains associated with growing autophagosomes. As such, two indicators of  
325 autophagy are elevated Atg8-II levels relative to Atg8-I and increased formation of  
326 Atg8+ autophagosome puncta. Because antibodies are not available to detect  
327 endogenous *M. brevicollis* autophagy markers or cargo receptors, we generated wild  
328 type and *STING*<sup>-</sup> cell lines stably expressing mCherry-Atg8. Stable expression of  
329 mCherry-Atg8 under the control of the constitutive pEFL promoter did not alter the  
330 relative susceptibilities of these cell lines to 2'3'cGAMP (Figure 6 - figure supplement  
331 1A). By immunoblot, mCherry-Atg8-II can be distinguished from mCherry-Atg8-I based  
332 on its enhanced gel mobility. When we exposed both cell lines to 2'3' cGAMP for three  
333 hours, we observed increased levels of Atg8-II relative to Atg8-I by immunoblot in wild  
334 type, but not *STING*<sup>-</sup> cells (Figure 6A). These results suggest that treatment with 2'3'  
335 cGAMP induces autophagic signaling in a *STING*-dependent manner; however, making  
336 this conclusion requires evidence of autophagy induction through inhibitor studies. To  
337 confirm autophagy induction, we treated cells with chloroquine, a lysosomotropic agent  
338 which inhibits autophagy by blocking endosomal acidification, thereby preventing  
339 amphisome formation and Atg8-II turnover<sup>54</sup>. Exposing wild type cells pretreated with  
340 chloroquine to 2'3' cGAMP for three hours resulted in increased levels of Atg8-II relative  
341 to Atg8-I, suggesting that 2'3' cGAMP treatment indeed induces the autophagic  
342 pathway (Figure 6B, Figure 6 - figure supplement 1B). In cells pretreated with  
343 chloroquine, *STING* levels did not markedly increase after exposure to 2'3' cGAMP  
344 (Figure 6 - figure supplement 1B), raising the possibility that the autophagic pathway is  
345 important for regulating *STING* protein levels. We next examined whether 2'3' cGAMP  
346 induces Atg8+ puncta formation by treating wild type and *STING*<sup>-</sup> cells with 2'3' cGAMP  
347 for three hours, and observing mCherry foci by microscopy (Figure 6C-F). Quantifying  
348 images revealed that Atg8+ puncta accumulate after 2'3' cGAMP treatment in wild type,  
349 but not *STING*<sup>-</sup> cells (Figure 6G). Overall, these results suggest that *M. brevicollis*  
350 responds to 2'3' cGAMP through *STING*-dependent induction of the autophagy  
351 pathway.

352 Finally, we asked whether *STING*-mediated autophagic pathway induction affects  
353 survival after exposure to 2'3' cGAMP (Figure 6H). To determine if inhibiting autophagy  
354 impacts 2'3' cGAMP-induced cell death, we examined the survival responses of wild  
355 type and *STING*<sup>-</sup> *M. brevicollis* to 2'3' cGAMP after pretreatment with lysosomotropic  
356 agents chloroquine or NH<sub>4</sub>Cl. Chloroquine or NH<sub>4</sub>Cl pretreatment rescued 2'3' cGAMP-  
357 induced cell death in wild type *M. brevicollis* (Figure 6H), whereas the survival of  
358 *STING*<sup>-</sup> cells, which are already resistant to 2'3' cGAMP-induced cell death, was not

359 affected. Therefore, we hypothesize that 2'3' cGAMP induces cell death in *M. brevicollis*  
360 by overstimulating STING-mediated autophagic signaling.

361

## 362 Discussion

363

364 Investigating choanoflagellate immune responses has the potential to inform the  
365 ancestry of animal immune pathways. In this study, we screened diverse bacteria to  
366 identify a choanoflagellate pathogen, and determined that *M. brevicollis* is killed by  
367 sustained exposure to *P. aeruginosa* bacteria. We found that STING, a crucial  
368 component of animal innate responses to cytosolic DNA, is upregulated in *M. brevicollis*  
369 after exposure to *P. aeruginosa* or the STING ligand 2'3' cGAMP. The application of  
370 newly-developed transgenic and genetic tools for *M. brevicollis* revealed that, similar to  
371 mammalian STING, *M. brevicollis* STING localizes to perinuclear endoplasmic reticulum  
372 regions. In addition, STING mediates responses to *P. aeruginosa* bacteria, and is  
373 required for inducing transcriptional changes and autophagic signaling in response to  
374 2'3' cGAMP. These data reveal that STING plays conserved roles in choanoflagellate  
375 immune responses, and provide insight into the evolution of STING signaling on the  
376 animal stem lineage.

377 The discovery that *M. brevicollis* STING mediates immune responses raises a  
378 number of interesting questions about the full extent of its physiological roles in  
379 choanoflagellates. For example, while our results demonstrate that *M. brevicollis* STING  
380 responds to exogenous 2'3' cGAMP, the endogenous triggers of STING activation in *M.*  
381 *brevicollis* remain to be determined. *M. brevicollis* has a putative cGAS homolog,  
382 suggesting that STING may respond to an endogenously produced cyclic dinucleotide  
383 similar to 2'3' cGAMP. Determining the enzymatic activities of *M. brevicollis* cGAS and  
384 identifying the endogenous trigger of *M. brevicollis* STING will be critical steps towards  
385 elucidating mechanisms of STING activation. Although cGAS and STING are rare  
386 among sequenced choanoflagellate species, both species with STING homologs, *M.*  
387 *brevicollis* and *S. macrocollata*, also harbor a cGAS homolog (Figure 1- Supplement  
388 1A), suggesting the presence of an intact choanoflagellate cGAS-STING pathway.

389 Our results suggest that *M. brevicollis* has distinct responses to 2'3' cGAMP  
390 versus 3'3'-linked cyclic dinucleotides produced by bacteria (Figure 3C,D, Figure 3 -  
391 figure supplement 1). In contrast to 2'3' cGAMP, bacterial cyclic dinucleotides (3'3'  
392 cGAMP, c-di-AMP, c-di-GMP) do not induce cell death in *M. brevicollis*. However, 3'3'  
393 cGAMP induces a robust transcriptional response in *M. brevicollis*, indicating that  
394 STING, or a different cyclic dinucleotide receptor<sup>57</sup>, responds to these bacterial  
395 molecules. One hypothesis is that *M. brevicollis* STING, similar to animal STING  
396 proteins<sup>14</sup>, may have different binding affinities for 2'3' and 3'3'-linked cyclic  
397 dinucleotides. It is also possible that bacterial cyclic dinucleotides activate additional  
398 pathways that influence survival in *M. brevicollis*. As bacterivores, choanoflagellates

399 likely benefit from a fine-tuned response to bacterial cyclic dinucleotides that enables  
400 them to interpret higher and lower concentrations in their environment. Elucidating  
401 mechanisms of STING activation in *M. brevicollis* could help reveal how STING proteins  
402 in animals evolved to respond to both bacterially-produced and endogenous cyclic  
403 dinucleotides.

404 While it is clear that 2'3' cGAMP stimulates STING-dependent transcriptional  
405 responses and autophagic signaling in *M. brevicollis* (Figure 5, Figure 6), the signaling  
406 pathways downstream of STING in choanoflagellates are unknown. Much of what is  
407 known about STING signaling comes from mammals and involves the extended CTT  
408 domain of STING, which *M. brevicollis* lacks, and immune genes that are restricted to  
409 vertebrates. Two pathways downstream of STING activation that are conserved in  
410 invertebrates, and as such are proposed ancestral functions of STING, are autophagy  
411 and NF- $\kappa$ B signaling. Here, we observed that STING is required for induction of the  
412 autophagy pathway in response to 2'3' cGAMP in *M. brevicollis*, indicating that the role  
413 of STING in regulating autophagy predates animal origins. While exposure to 2'3'  
414 cGAMP leads to NF- $\kappa$ B activation in the sea anemone *N. vectensis*<sup>58</sup> and in insects<sup>59–62</sup>,  
415 neither *M. brevicollis* nor *S. macrocollata*, the two choanoflagellate species with STING,  
416 possess a NF- $\kappa$ B homolog<sup>3</sup>. Nonetheless, 2'3' cGAMP activates an extensive  
417 transcriptional response downstream of STING in *M. brevicollis*, although the specific  
418 signaling pathways remain to be identified. This does not negate the hypothesis that  
419 STING signaling led to NF- $\kappa$ B activation in the Urmetazoan, but strongly suggests that  
420 additional pathways exist downstream of STING activation in choanoflagellates, and  
421 potentially in animals.

422 Choanoflagellates forage on diverse environmental bacteria for sustenance, yet  
423 how they recognize and respond to pathogens is a mystery. Our finding that *P.*  
424 *aeruginosa* has pathogenic effects on *M. brevicollis* (Figure 1) provides a much-needed  
425 framework for uncovering mechanisms of pathogen recognition and antibacterial  
426 immunity in choanoflagellates. Profiling the host transcriptional response to *P.*  
427 *aeruginosa* has allowed us to identify choanoflagellate genes that may be involved in  
428 recognizing (C-type lectins) and combating (polysaccharide lyases, antimicrobial  
429 peptides) bacteria; yet, it has also revealed the immense complexity of this interaction,  
430 with more than 600 *M. brevicollis* genes differentially expressed in response *P.*  
431 *aeruginosa*. Thus, identifying specific *P. aeruginosa* virulence factors will be critical for  
432 understanding why *P. aeruginosa* – but not other bacteria – have pathogenic effects on  
433 *M. brevicollis*, and facilitate the characterization of mechanisms underlying  
434 choanoflagellate pathogen responses.

435 With the establishment of molecular genetic techniques in choanoflagellates --  
436 first for *S. rosetta*<sup>50,52</sup>, and here for *M. brevicollis* -- we now have the opportunity to  
437 explore the functions of candidate immune genes. Identifying additional  
438 choanoflagellate pathogens, particularly viral pathogens, will also be key to delineating

439 immune response pathways. Finally, as choanoflagellates are at least as genetically  
440 diverse as animals<sup>3</sup>, expanding studies of immune responses to diverse  
441 choanoflagellate species will be essential for reconstructing the evolution of immune  
442 pathways in animals.

443  
444  
445  
446

#### Acknowledgements

447 We thank Bill Jackson, Tera Levin, Shally Margolis, Russell Vance, and Nan Yan  
448 for helpful advice and/or comments on the manuscript, and David Greenberg, David  
449 Hendrixson, Andrew Koh, Kim Orth, Russell Vance, and Sebastian Winter for bacterial  
450 strains. We thank Neal Alto for use of the widefield microscope, Monika Sigg for use of  
451 a reporter construct, and Mya Breitbart for sea water samples. We are grateful for David  
452 Booth's invaluable advice on developing transfection and gene editing protocols.

453 This work was funded by a Pew Innovation Fund award (JKP and NK), a HHMI  
454 Hanna Gray Fellows award (AW), a HHMI Faculty Scholar award (JKP), and a  
455 Burroughs Wellcome Fund Investigators in the Pathogenesis of Infectious Diseases  
456 (JKP). We acknowledge the assistance of the UT Southwestern Live Cell Imaging  
457 Facility, a Shared Resource of the Harold C. Simmons Cancer Center, supported in part  
458 by an NCI Cancer Center Support Grant, 1P30 CA142543-01.

459  
460  
461  
462  
463

#### Materials and Methods

<b>Key Resources Table</b>				
<b>Reagent type (species) or resource</b>	<b>Designation</b>	<b>Source or reference</b>	<b>Identifiers</b>	<b>Additional information</b>
Strain, strain background ( <i>M. brevicollis</i> )	<i>M. brevicollis</i>	ATCC PRA-258	PMID: 18276888	
Genetic reagent, ( <i>M. brevicollis</i> )	<i>M. brevicollis</i> STING <sup>-</sup>	This study		STING <sup>-</sup> knockout strain ; cell line maintained

				by A. Woznica
Transfected construct ( <i>M. brevicollis</i> )	pEFL5'-pac-P2A-STING-mTFP-3'act	This study		Construct to express <i>M. brevicollis</i> STING fused to mTFP; can be obtained from A. Woznica
Transfected construct ( <i>M. brevicollis</i> )	pEFL5'-pac-P2A-mCherry-Atg8--3'act	This study		Construct to express mCherry fused to <i>M. brevicollis</i> Atg8; can be obtained from A. Woznica
Strain, strain background( <i>Flavobacterium</i> )	<i>Flavobacterium</i> sp.	This study		Isolated from MX1 (ATCC PRA-258) culture; can be obtained from A. Woznica
Strain, strain background( <i>Pseudomonas aeruginosa</i> )	PAO1	ATCC 15692	PMID: 13961373	
<i>P. aeruginosa</i> , transgenic strain	PAO1-GFP	ATCC 15692GFP	PMID: 9361441	
Antibody	anti-choano STING (rabbit polyclonal)	This study		Generated by Pacific Immunology; dilution 1:200 for IF, 1:2000 dilution for

				WB; can be obtained from A. Woznica
antibody	Anti-mCherry 16D7 (rat monoclonal)	Invitrogen	Cat# M11217	1:2000 dilution for WB
antibody	Anti-human Tubulin E7 (Mouse monoclonal)	Developmental Studies Hybridoma Bank	Cat# <del>AB_231553</del> 3	1:200 dilution for IF
antibody	Alpha-human tubulin (Mouse monoclonal)	Sigma Aldrich	Cat # T64074	1:7000 dilution for WB
Chemical compound, drug	2'3' cGAMP	Cayman Chemical	Cat# 19887	
Chemical compound, drug	3'3' cGAMP	Cayman chemical	Cat# 17966	
Sequence-based reagent	<i>STING556</i> gRNA	This study	Guide RNA	TTTCGGGATT CAGATGTGG G
Sequenced-based reagent	<i>STING</i> locus PCR primers	This study	PCR primers	F: 5' ATG ATG GTT AAT CTC TCT GAT CTT TCA CAT C 3' R: 5' TTA TGG CAT CGC ATA CTG GTC C 3'

Commercial assay, kit	SG Cell Line 4D-NucleofectorT M X Kit S	Lonza,	Cat# V4XC-3032	
-----------------------	---	--------	----------------	--

464  
465  
466

#### Culturing choanoflagellates

467 All strains of *M. brevicollis* were co-cultured with *Flavobacterium sp.* bacteria<sup>4</sup>  
468 (American Type Culture Collection [ATCC], Manassas, VA; Cat. No. PRA-258) in a  
469 seawater based media enriched with glycerol, yeast extract, peptone and cereal grass  
470 (details in Media Recipes). Cells were grown either at room temperature, or at 16°C in a  
471 wine cooler (Koldfront). All *M. brevicollis* cell lines were verified by 18S sequencing and  
472 RNA-seq. Choanoflagellate cell lines *S. rosetta*, *S. macrocollata*, *S. punica*, and *S.*  
473 *infusionum* were verified by 18S sequencing.

474

#### Bacterial effects on *M. brevicollis*

##### ***Isolating environmental bacteria***

476 Environmental bacterial species were isolated from water samples from Woods  
477 Hole, MA, St. Petersburg, FL, and Dallas, TX. Water samples were streaked onto Sea  
478 Water Complete media or LB plates, and grown at 30° C or 37° C. After isolating  
479 individual colonies, partial 16S sequencing using 16S universal primers (27F: 5'-  
480 AGAGTTTGATCCTGGCTCAG-3', 1492R: 5'-TACGGYTACCTTGTTACGACTT-3') was  
481 used to determine the identity of the bacterial isolates.

##### ***Screening for pathogenic effects***

482 *M. brevicollis* was grown for 30 h, and feeding bacteria were reduced through  
483 one round of centrifugation and resuspension in artificial seawater (ASW). Cells were  
484 counted on a hemocytometer and diluted to 5x10<sup>6</sup> cells/mL in High Nutrient Medium,  
485 and plated into 24-well plates.

486 For each bacterium, a single colony was inoculated into LB and grown shaking  
487 overnight at either 30° C (environmental isolates) or 37° C (mouse isolates). Bacterial  
488 cells were pelleted by centrifugation for 5 minutes at 4000 x g, and resuspended in  
489 artificial seawater (ASW) to an OD~1.

490 Each bacterial species was added to *M. brevicollis* culture at two concentrations  
491 (10mL/mL and 50 mL/mL) in duplicate. *M. brevicollis* was then monitored at regular  
492 intervals for changes in behavior and growth.

##### ***Growth curves in the presence of bacteria***

493 All bacteria were grown shaking at 30° C in Sea Water Complete media or LB (to  
494 optical density of 0.8). For each bacterial strain, CFU plating was used to estimate the  
495 number of bacterial cells/ mL under these growth conditions. To prepare bacterial  
496 conditioned media, bacterial cells were pelleted by centrifugation for 10 minutes at 4000  
497 x g, and supernatant was passed through a 0.22mm sterilizing filter.

500



501 *M. brevicollis* was grown for 30 h, and bacteria were washed away through two  
502 consecutive rounds of centrifugation and resuspension in artificial seawater (ASW).  
503 Cells were counted on a hemocytometer and diluted to  $1.0 \times 10^6$  cells/mL (growth curves  
504 with live bacteria) or  $1.5 \times 10^5$  cells/mL (growth curves with conditioned medium) in High  
505 Nutrient Medium. To test the effects of live bacteria,  $1.5 \times 10^6$  bacterial cells were added  
506 per 1 mL of *M. brevicollis* culture. To test the effects of bacterial conditioned media, 50  
507 ml of bacterial conditioned media was added per 1 mL of *M. brevicollis* culture. For each  
508 growth curve biological replicate, cells were plated into 24-well plates, and two wells  
509 were counted per time point as technical replicates. At least three biological replicates  
510 are represented in each graph.

### 511 **Bacterial internalization**

512 Fluorescent *E. coli* and *P. aeruginosa* were grown shaking at 30° C in LB to an  
513 optical density of  $OD_{600}=0.8$ . Fluorescent *C. jejuni* was grown from freezer stocks in  
514 microaerobic conditions on Mueller-Hinton agar. For each bacterial strain, CFU plating  
515 was used to estimate the number of bacterial cells/ mL under these growth conditions.

516 *M. brevicollis* was grown for 30 h, and feeding bacteria were washed away with  
517 one round of centrifugation and resuspension in artificial seawater (ASW). Cells were  
518 counted and diluted to  $1.5 \times 10^5$  cells/mL in ASW.  $1.5 \times 10^7$  bacterial cells were added to 2  
519 mL *M. brevicollis* culture (MOI=50), and co-incubated at room temperature for 1 hr with  
520 gentle mixing at regular intervals to avoid settling. To quantify bead internalization, *M.*  
521 *brevicollis* was co-incubated with bacteria for 1 hour (as described above), at which  
522 point  $\sim 1 \times 10^{10}$  beads (0.2mm diameter, resuspended in 1% BSA to prevent clumping)  
523 were added to the conical for an additional 30 minutes.

524 Prior to imaging, 200mL aliquots were transferred to 8-well glass bottom  
525 chambers (Ibidi Cat. No 80827). Live imaging was performed on a Zeiss Axio Observer  
526 widefield microscope using a 63x objective. Images were processed and analyzed using  
527 Fiji<sup>63</sup>.

### 528 ***P. aeruginosa* deletion mutants**

529 *P. aeruginosa* deletion strains were acquired from the Seattle PAO1 transposon  
530 mutant library (NIH P30 DK089507). Strains RP436 and RP576 (PMID 15731071) were  
531 acquired from Russell Vance, The effects of both live bacteria and bacterial conditioned  
532 medium were tested for all acquired strains at a range of PFU/mL (live bacteria) or  
533 percent volume (conditioned medium).

534

### 535 Immune agonist dose-response curves

536 *M. brevicollis* was grown to late-log phase, and feeding bacteria were reduced  
537 through one round of centrifugation and resuspension in artificial seawater (ASW). Cells  
538 were counted on a hemocytometer and diluted to  $1.0 \times 10^6$  cells/mL (growth curves with  
539 live bacteria) in High Nutrient Medium, and aliquoted into 96-well (100µL/well) or 24-well  
540 (1mL/well) plates. Immune agonists were added at indicated concentrations in technical  
541 duplicate, and cells were counted again after 24 hours. % survival is a calculation of:

542 [mean experimental (cells/mL) / mean control (cells/mL)]. Each dose-response curve is  
543 representative of at least three biological replicates.

544

#### 545 RNA-seq

##### 546 ***Growth of choanoflagellate cultures***

547 After thawing new cultures, growth curves were conducted to determine the  
548 seeding density and time required to harvest cells at late-log phase growth. To grow  
549 large numbers of cells for RNA-seq, cells were seeded one to two days prior to the  
550 experiment in either 3-layer flasks (Falcon; Corning, Oneonta, NY, USA; Cat. No. 14-  
551 826-95) or 75 cm<sup>2</sup> flasks (Falcon; Corning, Oneonta, NY, USA; Cat. No. 13-680-65),  
552 and grown at room temperature. Bacteria were washed away from choanoflagellate  
553 cells through two rounds of centrifugation and resuspension in artificial seawater (ASW).  
554 To count the cell density, cells were diluted 100-fold in 200 µl of ASW, and fixed with 1  
555 µL of 16% paraformaldehyde. Cells were counted on a hemocytometer, and the  
556 remaining cells were diluted to a final concentration of 4×10<sup>6</sup> choanoflagellate cells/mL.  
557 The resuspended cells were divided into 2.5 mL aliquots and plated in 6-well plates  
558 prior to treatment. After treatment, cells were transferred to a 15 mL conical and  
559 pelleted by centrifugation at 2400 x g for 5 min, flash frozen with liquid nitrogen, and  
560 stored at -80°C.

##### 561 ***RNA isolation***

562 Total RNA was isolated from cell pellets with the RNAqueous kit (Ambion,  
563 Thermo Fisher Scientific). Double the amount of lysis buffer was used to increase RNA  
564 yield and decrease degradation, and RNA was eluted in minimal volumes in each of the  
565 two elution steps (40 µL and 15 µL). RNA was precipitated in LiCl to remove  
566 contaminating genomic DNA. Total RNA concentration and quality was evaluated using  
567 the Agilent Bioanalyzer 2100 system and RNA Nano Chip kit (Cat No. 5067-1511).

##### 568 ***Library preparation, sequencing, and analysis***

569 Libraries were prepared and sequenced by the UTSW Genomics Sequencing  
570 Core. RNA libraries were generated with the Illumina TruSeq® Stranded mRNA Library  
571 prep kit (Cat No. 20020594), using a starting total RNA input of 2-3 µg. To remove  
572 contaminating bacterial RNA, samples were first poly-A selected using oligo-dT  
573 attached magnetic beads. Following purification, the mRNA was fragmented at 94°C for  
574 4 minutes, and cleaved RNA fragments were synthesized into cDNA. After an end  
575 repair step, UMI adapters (synthesized by IDT) were ligated to the cDNA, and the  
576 products were twice purified using AMPure XP beads before amplification.  
577 Library quantity was measured using the Quant-iT™ PicoGreen dsDNA Assay kit by  
578 Invitrogen (Cat No. P7589) and a PerkinElmer Victor X3, 2030 Multilabel Reader.  
579 Library quality was verified on an Agilent 2100 Bioanalyzer instrument using Agilent  
580 High sensitivity DNA kit (Cat No. 5067-4626) or DNA 1000 kit (Cat No. 5067-  
581 1504). Libraries were pooled, and sequenced in different batches on either the Illumina

582 NextSeq 550 system with SE-75 workflow, or the Illumina NovaSeq 6000 system with  
583 S4 flowcell and XP PE-100 workflow, generating 25-40 million reads per sample. Reads  
584 were checked for quality using fastqc (v0.11.2) and fastq\_screen (v0.4.4), and trimmed  
585 using fastq-mcf (ea-utils, v1.1.2-806). Trimmed fastq files were mapped to the *Monosiga*  
586 *brevicollis* reference genome (NCBI:txid81824) using TopHat<sup>64</sup> (v2.0.12). Duplicates  
587 were marked using picard-tools (v2.10.10). Read counts were generated using  
588 featureCounts<sup>65</sup>, and differential expression analysis was performed using edgeR<sup>66</sup>.  
589 Statistical cutoffs of  $FDR \leq 10^{-4}$  were used to identify significant differentially expressed  
590 genes. GO enrichment analysis of differentially expressed genes was performed using  
591 DAVID (<https://david.ncifcrf.gov/>).

592

### 593 RT-qPCR

594 RNA was isolated as described above, and cDNA was synthesized from total  
595 RNA with the High Capacity cDNA Reverse Transcription kit (Applied Biosystems;  
596 Thermo Fisher. Real-time PCR was performed with iTaq Universal SYBR Green  
597 Supermix (Biorad; Cat No. 1725121) or SYBR Green PCR master mix (Applied  
598 Biosystems; Cat No. 4309155) in either an 7500 Fast Real-Time PCR System (Applied  
599 Biosystems), or a QuantStudio 3 Real-Time PCR System (Applied Biosystems). Ct  
600 values were converted into relative gene expression using the  $\Delta\Delta C_t$  method (Livak and  
601 Schmittgen, 2001) and the internal control gene RPL15 (MONBRDRAFT\_38309).

602

### 603 Immunoblotting

604 *M. brevicollis* was harvested by centrifugation at 5,000 x g for 5 min at 4°C, and  
605 resuspended in 100  $\mu$ L lysis buffer (50mM Tris, pH 7.4, 150 mM NaCl, 1 mM EDTA, 1  
606 mM ethyleneglycoltetraacetic acid [EGTA], 0.5% sodium deoxycholate, 1% NP-40)  
607 containing protease inhibitor cocktail (Roche) for 10 min at 4°C. The crude lysate was  
608 clarified by centrifugation at 10,000 x g for 10 min at 4°C, and denatured in Laemmli  
609 buffer before SDS-PAGE. Proteins were transferred to an Immobilon-P PVDF  
610 membrane (Millipore), and blocked for two hours in PBST (1x PBS containing 5% nonfat  
611 dry milk and 0.05% Tween-20). Membranes were incubated with primary antibodies  
612 diluted in PBST overnight at 4°C and washed extensively in PBST. Membranes were  
613 incubated with secondary antibodies for 1 hour at room temperature, washed  
614 extensively in PBST, and developed using Immobilon Western Chemiluminescent HRP  
615 Substrate (Millipore Sigma). Source data files for all western blots are provided as  
616 Source Data File 1.

### 617 **STING antibody production**

618 The anti-mbreSTING antibody was generated by Pacific Immunology. Rabbits  
619 were immunized with a KLH-conjugated peptide corresponding to residues 320-338 of  
620 *M. brevicollis* protein EDQ90889.1 (Cys-KNRSEVLKMKMRAEDQYAMP), and serum was  
621 affinity purified against the peptide to reduce cross-reactivity and validated using  
622 immunoblotting.

623

#### 624 Immunofluorescence Staining and Imaging

625 Depending on the cell density of the starting culture, between 0.2-1 mL of cells  
626 were concentrated by centrifugation for 5 min at 2500 × g. The cells were resuspended  
627 in 200 µl of artificial seawater and applied to poly-L-lysine-coated coverslips (Corning  
628 Life Sciences; Cat. No.354085) placed at the bottom of each well of a 24-well cell  
629 culture dish. After the cells were allowed to settle on the coverslip for 30 min, 150 µl of  
630 the cell solution was gently removed from the side of the dish. All of the subsequent  
631 washes and incubations during the staining procedure were performed by adding and  
632 removing 200 µl of the indicated buffer.

633 Cells were fixed in two stages. First, 200 µl cold 6% acetone diluted in 4X PBS  
634 was added for 5 min at room temperature. Next, 200 µl cold 8% paraformaldehyde  
635 diluted in 4X PBS was added (yielding a final concentration of 4% paraformaldehyde),  
636 and the fixative mixture was incubated for 15 min at room temperature. After fixation,  
637 the coverslip was gently washed three times with 200 µl 4X PBS.

638 Cells were permeabilized by incubating in permeabilization buffer (4X PBS; 3%  
639 [wt/vol] bovine serum albumin (BSA)-fraction V; 0.2% [vol/vol] Triton X-100) for 30 min.  
640 After removing permeabilization buffer, the coverslip was incubated in primary antibody  
641 for 1 hour at room temperature, and then washed three times in 4X PBS. The coverslip  
642 was then incubated with secondary antibody for 1 hour at room temperature, and then  
643 washed twice in 4X PBS. The coverslip was next incubated in 4 U/ml Phalloidin  
644 (Thermo Fisher Scientific) for 30 min at room temperature, washed once in 4X PBS.  
645 Lastly, the coverslip was incubated in 10 µg/ml Hoechst 33342 (Thermo Fisher  
646 Scientific) for 5 min at room temperature, and then washed once with 4X PBS.

647 To prepare a slide for mounting, 10 µl of Pro-Long Gold (Thermo Fisher  
648 Scientific) was added to a slide. The coverslip was gently removed from the well with  
649 forceps, excess buffer was blotted from the side with a piece of filter paper, and the  
650 coverslip was gently placed on the drop of Pro-Long diamond. The mounting media  
651 cured overnight before visualization.

652 Images were acquired on either: (1) a Zeiss LSM 880 Airyscan confocal microscope  
653 with a 63x objective by frame scanning in the superresolution mode (images processed  
654 using the automated Airyscan algorithm (Zeiss)), or (2) a Nikon CSU-W1 SoRa spinning  
655 disk confocal microscope with a 60x objective in SR mode (images processed using  
656 Imaris).

657

#### 658 Live-Cell Imaging

659 Cells transfected with fluorescent reporter plasmid were prepared for microscopy  
660 by transferring 200 µl of cells to a glass-bottom dish or glass-bottom 8-well chamber  
661 (Ibidi). Confocal microscopy was performed on a Zeiss Axio Observer LSM 880 with an  
662 Fast Airyscan detector and a 63x/NA1.40 Plan-Apochromatic oil immersion objective

663 (Carl Zeiss AG, Oberkochen, Germany). Confocal stacks were acquired by frame  
664 scanning in superresolution mode, and images were processed using the automated  
665 Airyscan algorithm (Zeiss).

666

#### 667 Transfection of *M. brevicollis*

668 **Cell Culture.** One day prior to transfection, 60 ml of High Nutrient Medium was  
669 inoculated with *M. brevicollis* to a final concentration of 10000 cells/ml. The culture was  
670 split in two, and grown in two 75 cm<sup>2</sup> flasks at room temperature, approximately 22°C  
671 (Falcon; Corning, Oneonta, NY, USA; Cat. No. 13-680-65).

672 **Cell Washing.** After 24 hours of growth, bacteria were washed away from *M.*  
673 *brevicollis* cells through three consecutive rounds of centrifugation and resuspension in  
674 artificial seawater (ASW). The culture flasks were combined and vigorously shaken for  
675 30 s, and then transferred to 50-ml conical tubes and spun for 5 min at 2000 × *g* and  
676 22°C. The supernatant was removed with a serological pipette, and residual media were  
677 removed with a fine-tip transfer pipette. The cell pellets were resuspended in a single  
678 conical tube in a total volume of 50 ml of ASW, vigorously shaken for 30 s, and then  
679 centrifuged for 5 min at 2050 × *g*. The supernatant was removed as before. In a final  
680 washing step, the cell pellet was resuspended in 50 mL ASW, shaken vigorously, and  
681 centrifuged for 5 min at 2100 × *g*. After the supernatant was removed, the cells were  
682 resuspended in a total volume of 400 µl of ASW. To count the cell density, cells were  
683 diluted 100-fold in 200 µl of ASW, and fixed with 1 µl of 16% paraformaldehyde. Cells  
684 were counted on a hemocytometer, and the remaining cells were diluted to a final  
685 concentration of 5 × 10<sup>7</sup> choanoflagellate cells/ml. The resuspended cells were divided  
686 into 100-µl aliquots with 5 × 10<sup>6</sup> cells per aliquot to immediately prime cells in the next  
687 step.

688 **Cell Priming.** Each aliquot of *M. brevicollis* cells was incubated in priming buffer (40  
689 mM HEPES-KOH, pH 7.5; 55 mM lithium citrate; 50 mM L-cysteine; 10% [wt/vol] PEG  
690 8000; and 2 µM papain) to remove the extracellular material coating the cell. The 100-µl  
691 aliquots, which contained 5 × 10<sup>6</sup> cells, were centrifuged for 5 min at 1700 × *g*. The  
692 supernatant was removed, and cells were resuspended in 100 µl of priming buffer and  
693 then incubated for 35 min at room temperature. Priming was quenched by adding 4 µl of  
694 50-mg/ml bovine serum albumin-fraction V (Thermo Fisher Scientific, Waltham, MA;  
695 Cat. No. BP1600-100) and then centrifuged for 5 min at 1250 × *g* and 22°C with the  
696 centrifuge brake set to a “soft” setting. The supernatant was removed with a fine-tip  
697 micropipette, and the cells were resuspended in 25 µl of SG Buffer (Lonza).

698 **Nucleofection.** Each transfection reaction was prepared by adding 2 µl of “primed”  
699 cells resuspended in SG buffer (Lonza) to a mixture of: 16 µl of SG buffer, 2 µl of 20  
700 µg/µl pUC19, 1 µl of 250 mM ATP (pH 7.5), 1 µl of 100 mg/ml sodium heparin, and ≤7 µl  
701 of reporter DNA (volume is dependent on the number of constructs transfected). Each  
702 transfection reaction was transferred to one well in 16-well nucleofection strip (Lonza;

703 Cat. No. V4XC-2032). The nucleofection strip was placed in the X-unit (Lonza; Cat. No.  
704 AAF-1002F) connected to a Nucleofector 4D core unit (Lonza; Cat. No. AAF-1002B),  
705 and the EO100 pulse was applied to each well.

706 **Recovery.** 100 µl of cold recovery buffer (10 mM HEPES-KOH, pH 7.5; 0.9 M  
707 sorbitol; 8% [wt/vol] PEG 8000) was added to the cells immediately after pulsation. After  
708 5 minutes, the whole volume of the transfection reaction plus the recovery buffer was  
709 transferred to 2 ml of Low Nutrient Medium in a 12-well plate. The cells were grown for  
710 24–48 hours before being assayed for luminescence or fluorescence.

711 **Puromycin Selection.** To generate stably transfected *M. brevicollis* cell lines,  
712 puromycin was added to cells 24 hours after transfection at a final concentration of 300  
713 µg/mL. Cells were monitored over the course of 7-21 days, and fresh High Nutrient  
714 Media + 300 µg/mL puromycin was added to the cells as needed.

715

### 716 Genome editing

717 For a more detailed description of gRNA and repair oligonucleotide design, refer to  
718 Booth et al. 2018<sup>50</sup>.

719 **Design and preparation of gRNAs** First, crRNAs were designed by using the  
720 extended recognition motif 5'-HNNGRSGGH-3' (in which the PAM is underlined, N  
721 stands for any base, R stands for purine, S stands for G or C, and H stands for any  
722 base except G) to search for targets in cDNA sequences<sup>67</sup>. Next, we confirmed that the  
723 RNA sequence did not span exon-exon junctions by aligning the sequence to genomic  
724 DNA.

725 Functional gRNAs were prepared by annealing synthetic crRNA with a synthetic  
726 tracrRNA<sup>52</sup>. To prepare a functional gRNA complex from synthetic RNAs, crRNA and  
727 tracrRNA (Integrated DNA Technologies [IDT], Coralville, IA, USA) were resuspended  
728 to a final concentration of 200 µM in duplex buffer (30 mM HEPES-KOH, pH 7.5; 100  
729 mM potassium acetate; IDT, Cat. No. 11-0103-01). Equal volumes of crRNA and  
730 tracrRNA stocks were mixed together, incubated at 95°C for 5 min in an aluminum  
731 block, and then the entire aluminum block was placed at room temp to slowly cool the  
732 RNA to 25°C. The RNA was stored at -20°C

733 **Design and preparation of repair oligonucleotides** Repair oligonucleotides for  
734 generating knockouts were designed by copying the sequence 50 bases upstream and  
735 downstream of the SpCas9 cleavage site. A knockout sequence  
736 (5'TTTATTTAATTAAATAAA-3') was inserted at the cleavage site<sup>52</sup>.

737 Dried oligonucleotides (IDT) were resuspended to a concentration of 250 µM in a  
738 buffer of 10 mM HEPES-KOH, pH 7.5, incubated at 55°C for 1 hour, and mixed well by  
739 pipetting up and down. The oligonucleotides were stored at -20°C.

### 740 **Delivery of gene editing cargoes with nucleofection**

741 The method for delivering SpCas9 RNPs and DNA repair templates into *M.*  
742 *brevicollis* is as follows:

743 **Cell Culture.** One day prior to transfection, 60 ml of High Nutrient Medium was  
744 inoculated to a final concentration of *M. brevicollis* at 10000 cells/ml. The culture was  
745 split in two, and grown in two 75 cm<sup>2</sup> flasks at room temperature, approximately 22°C  
746 (Falcon; Corning, Oneonta, NY, USA; Cat. No. 13-680-65).

747 **Assembly of Cas9/gRNA RNP.** Before starting transfections, the *SpCas9* RNP was  
748 assembled. For one reaction, 2 µl of 20 µM *SpCas9* (NEB, Cat. No. M0646M) was  
749 placed in the bottom of a 0.25 ml PCR tube, and then 2 µl of 100 µM gRNA was slowly  
750 pipetted up and down with *SpCas9* to gently mix the solutions. The mixed solution was  
751 incubated at room temperature for 1 hour, and then placed on ice.

752 **Thaw DNA oligonucleotides.** Before using oligonucleotides in nucleofections, the  
753 oligonucleotides were incubated at 55°C for 1 hour.

754 **Cell Washing.** After 24 hours of growth, bacteria were washed away from *M.*  
755 *brevicollis* cells through three consecutive rounds of centrifugation and resuspension in  
756 artificial seawater (ASW). The culture flasks were combined and vigorously shaken for  
757 30 s, and then transferred to 50-ml conical tubes and spun for 5 min at 2000 × *g* and  
758 22°C. The supernatant was removed with a serological pipette, and residual media were  
759 removed with a fine-tip transfer pipette. The cell pellets were resuspended in a single  
760 conical tube in a total volume of 50 ml of ASW, vigorously shaken for 30 s, and then  
761 centrifuged for 5 min at 2050 × *g*. The supernatant was removed as before. In a final  
762 washing step, the cell pellet was resuspended in 50 mL ASW, shaken vigorously, and  
763 centrifuged for 5 min at 2100 × *g*. After the supernatant was removed, the cells were  
764 resuspended in a total volume of 400 µl of ASW. To count the cell density, cells were  
765 diluted 100-fold in 200 µl of ASW, and fixed with 1 µl of 16% paraformaldehyde. Cells  
766 were counted on a hemocytometer, and the remaining cells were diluted to a final  
767 concentration of 5 × 10<sup>7</sup> choanoflagellate cells/ml. The resuspended cells were divided  
768 into 100-µl aliquots with 5 × 10<sup>6</sup> cells per aliquot to immediately prime cells in the next  
769 step.

770 **Cell Priming.** Each aliquot of *M. brevicollis* cells was incubated in priming buffer (40  
771 mM HEPES-KOH, pH 7.5; 50 mM lithium citrate; 50 mM L-cysteine; 15% [wt/vol] PEG  
772 8000; and 2 µM papain) to remove the extracellular material coating the cell. The 100-µl  
773 aliquots, which contained 5 × 10<sup>6</sup> cells, were centrifuged for 5 min at 1700 × *g* and at  
774 room temperature. The supernatant was removed, and cells were resuspended in 100  
775 µl of priming buffer and then incubated for 35 min. Priming was quenched by adding 10  
776 µl of 50-mg/ml bovine serum albumin-fraction V (Thermo Fisher Scientific, Waltham,  
777 MA; Cat. No. BP1600-100). Cells were then centrifuged for 5 min at 1250 × *g* and 22°C  
778 with the centrifuge brake set to a “soft” setting. The supernatant was removed with a  
779 fine-tip micropipette, and the cells were resuspended in 25 µl of SG Buffer (Lonza).

780 **Nucleofection.** Each nucleofection reaction was prepared by adding 16 µl of cold  
781 SG Buffer to 4 µl of the *SpCas9* RNP that was assembled as described above. For  
782 reactions that used two different guide RNAs, each gRNA was assembled with *SpCas9*

783 separately and 4  $\mu$ l of each RNP solution were combined at this step. 2  $\mu$ l of the repair  
784 oligonucleotide template was added to the SpCas9 RNP diluted in SG buffer. Finally, 2  
785  $\mu$ l of primed cells were added to the solution with Cas9 RNP and the repair template.  
786 The nucleofection reaction was placed in one well of a 16-well nucleofection strip  
787 (Lonza; Cat. No. V4XC-2032). The nucleofection strip was placed in the X-unit (Lonza;  
788 Cat. No. AAF-1002F) connected to a Nucleofector 4D core unit (Lonza; Cat. No. AAF-  
789 1002B), and the EO100 pulse was applied to each well.

790 **Recovery.** 100  $\mu$ l of cold recovery buffer (10 mM HEPES-KOH, pH 7.5; 0.9 M  
791 sorbitol; 8% [wt/vol] PEG 8000) was added to the cells immediately after pulsation. After  
792 5 minutes, the whole volume of the transfection reaction plus the recovery buffer was  
793 transferred to 1 ml of High Nutrient Medium in a 12-well plate.

794 **Cycloheximide Selection in *M. brevicollis*.** One day after transfection, 10  $\mu$ l of 10  
795  $\mu$ g/ml cycloheximide was added per 1 mL culture of transfected cells. The cells were  
796 incubated with cycloheximide for 5 days prior to clonal isolation and genotyping.

797 **Genotyping.** Cells were harvested for genotyping by spinning 0.5ml of cells at  
798 4000g and 22°C for 5 min. The supernatant was removed and DNA was isolated either  
799 by Base-Tris extraction [in which the cell pellet was resuspended in 20uL base solution  
800 (25mM NaOH, 2mM EDTA), boiled at 100°C for 20 min, cooled at 4°C for 5 min, and  
801 neutralized with 20uL Tris solution (40mM Tris-HCl, pH 7.5)], or by DNAzol Direct [in  
802 which the cell pellet was resuspended in 50uL and incubated at room temperature for  
803 30 min (Molecular Research Center, Inc. [MRC, Inc.], Cincinnati, OH; Cat. No. DN131)].  
804 3  $\mu$ l of the DNA solution was added to a 25  $\mu$ l PCR reaction (DreamTaq Green PCR  
805 Master Mix, Thermo Fisher Scientific Cat No K1082) and amplified with 34 rounds of  
806 thermal cycling.

807

#### 808 Data Availability

809 Source data files for all western blots are provided in Source Data File 1. Raw  
810 sequencing reads and normalized gene counts for all RNA-seq experiments have been  
811 deposited at the NCBI GEO under accession GSE174340.

812

813

814



815 **Figure Legends**

816

817 **Figure 1. *P. aeruginosa* has pathogenic effects on *M. brevicollis***

818 **(A)** Immunofluorescence illuminates the diagnostic cellular architecture of *M. brevicollis*,  
819 including an apical flagellum (f) made of microtubules, surrounded by an actin-filled  
820 microvilli feeding collar (co). Staining for tubulin (green) also highlights cortical  
821 microtubules that run along the periphery of the cell body, and staining for F-actin  
822 (magenta) highlights basal filopodia (fp). DNA staining (blue) highlights the nucleus (n).

823 **(B)** *M. brevicollis* exhibits truncated flagella after exposure to *P. aeruginosa*. *M.*  
824 *brevicollis* were exposed to *E. coli* or *P. aeruginosa* for 24 hours, and then fixed and  
825 immunostained. Arrows point to flagella. Green: anti-tubulin antibody (flagella and cell  
826 body), magenta: phalloidin (collar), blue: Hoechst (bacterial and choanoflagellate  
827 nuclei). Scale bars represent 10 $\mu$ m. Flagellar length was quantified using Fiji, and  
828 statistical analysis (unpaired t-tests) was performed in GraphPad software. **(C)**

829 Exposure to *P. aeruginosa*, but not other Gammaproteobacteria, results in *M. brevicollis*  
830 cell death. Bacteria were added to *M. brevicollis* culture at an MOI of 1.5 (at Hours=0),  
831 and *M. brevicollis* cell density was quantified at indicated time points. Data represent  
832 mean  $\pm$  SD for three biological replicates. Statistical analysis (multiple unpaired t-tests)

833 was performed in GraphPad software; *p*-values shown are from comparisons between  
834 *Flavobacterium* and *P. aeruginosa*. **(D-F)** *M. brevicollis* does not ingest *P. aeruginosa*  
835 bacteria. **(D,E)** *M. brevicollis* were fed either fluorescent *E. coli* (D) or *P. aeruginosa* (E)  
836 for one hour, and then visualized by DIC (D,E, left) and green fluorescence (D, E, right).  
837 Fluorescent food vacuoles were observed in choanoflagellates fed *E. coli*, but not *P.*  
838 *aeruginosa*. **(F)** *M. brevicollis* was exposed to GFP-expressing *E. coli*, *V.*

839 *parahaemolyticus*, *C. jejuni*, or *P. aeruginosa* (MOI=50) for one hour, and then imaged  
840 by DIC and green fluorescence to quantify number of cells with internalized bacteria.  
841 Choanoflagellate cells with  $\geq 1$  GFP+ food vacuole were scored as GFP+, and cells  
842 without any GFP+ food vacuoles were scored as GFP-. Data represent cells quantified  
843 over three biological replicates. **(G,H)** *P. aeruginosa* does not broadly inhibit *M.*

844 *brevicollis* phagocytosis. **(G)** Internalization of 0.2 $\mu$ m fluorescent beads was used to  
845 quantify phagocytic activity after exposure to *E. coli* or *P. aeruginosa* bacteria. Although  
846 cells did not phagocytose *P. aeruginosa*, cells exposed to *E. coli* and *P. aeruginosa* had  
847 similar phagocytic uptake of beads. Data represent n=600 cells from three biological  
848 replicates. Statistical analyses (multiple unpaired t-tests) were performed in GraphPad  
849 software. **(H)** Exposure to *P. aeruginosa* does not inhibit phagocytic uptake of *E. coli*.

850 Internalization of fluorescent *E. coli* or *P. aeruginosa* bacteria was quantified after  
851 exposure to unlabeled *P. aeruginosa* (PAO1 strain). Data represent n=200 cells from  
852 two biological replicates. Statistical analysis (unpaired t-test) was performed in  
853 GraphPad software. **(I)** Secreted *P. aeruginosa* molecules are sufficient to induce *M.*  
854 *brevicollis* cell death. 5% (vol/vol) bacterial conditioned medium was added to *M.*

855 *brevicollis* culture (at Hours=0), and *M. brevicollis* cell density was quantified at  
856 indicated time points. Data represent mean +/- SD for three biological replicates.  
857 Statistical analysis (multiple unpaired t-tests) was performed in GraphPad software, and  
858 *p*-values shown are from comparisons between *Flavobacterium* and *P. aeruginosa*. **(J)**  
859 Sustained exposure to secreted *P. aeruginosa* molecules is required to induce *M.*  
860 *brevicollis* cell death. *P. aeruginosa* or *Flavobacterium* conditioned medium (5% vol/vol)  
861 was added to stationary-phase *M. brevicollis* cultures. After indicated times, cultures  
862 were washed and resuspended in fresh media. *M. brevicollis* cell density was quantified  
863 after 24 hours. The % survival is a measure of the cell density of *P. aeruginosa*-treated  
864 cells relative to *Flavobacterium*-treated controls. Data represent mean +/- SD for three  
865 biological replicates.

866  
867  
868

869 **Figure 1 – figure supplement 1. Presence of animal innate immune genes in**  
870 **choanoflagellates (A)** The transcriptomes of 21 choanoflagellate species<sup>3</sup> were  
871 searched for genes that play key roles in animal innate immune responses. Evidence  
872 for gene presence was based on sequence homology in a BLAST-based approach and  
873 conserved domain architectures, as described in Richter et al., 2018.

874

875 **Video 1, Supplementary file 1. *P. aeruginosa* influences *M. brevicollis* motility.**  
876 Movies depicting *M. brevicollis* cultures after exposure to *E. coli* or *P. aeruginosa*  
877 bacteria for 16 hours. In the absence of pathogenic bacteria, like *E. coli*, *M. brevicollis* is  
878 a highly motile flagellate and swims up in the water column. However, co-culturing *M.*  
879 *brevicollis* with *P. aeruginosa* results in reduced motility and cell settling.

880

881 **Figure 2. STING is upregulated in *M. brevicollis* after exposure to *P. aeruginosa***  
882 **(A,B)** *STING* transcript levels increase in response to *P. aeruginosa*. **(A)** Volcano plot  
883 displaying genes differentially expressed between *M. brevicollis* exposed to *P.*  
884 *aeruginosa* PAO1 and *Flavobacterium* (control) conditioned medium for three hours.  
885 Differentially expressed genes are depicted by blue (674 upregulated genes) and yellow  
886 (232 downregulated genes) dots (fold change $\geq$ 2; FDR $\leq$ 1e<sup>-4</sup>). Select genes that are  
887 upregulated or may function in innate immunity are labeled. RNA-seq libraries were  
888 prepared from four biological replicates. **(B)** After a three-hour treatment, *STING* mRNA  
889 levels (determined by RNA-seq) increase 1.42 fold in cells exposed to *Flavobacterium*  
890 conditioned medium and 5.54 fold in cells exposed to *P. aeruginosa* conditioned  
891 medium, compared to untreated controls. **(C)** *STING* protein levels increase after  
892 exposure to *P. aeruginosa*. *STING* levels were examined by immunoblotting at indicated  
893 timepoints after exposure to *Flavobacterium* or *P. aeruginosa* conditioned medium (5%  
894 vol/vol). Tubulin is shown as loading control, and intensity of *STING* protein bands were

895 quantified relative to tubulin. Statistical analysis (one-way ANOVA, Dunnett's multiple  
896 comparison) was performed in GraphPad software, and *p*-values shown are calculated  
897 using 0 hour timepoint as the control group.

898  
899  
900

901 **Figure 2 – figure supplement 2. *M. brevicollis* response to *P. aeruginosa*, and**  
902 **STING antibody validation and protein alignment. (A)** Gene ontology enrichment  
903 analysis of genes identified as differentially expressed (fold change $\geq$ 2; FDR $\leq$ 1e<sup>-4</sup>) after  
904 exposure to *P. aeruginosa*. Due to lack of annotation, >40% of the differentially  
905 expressed genes were not included in the enrichment analysis. **(B)** qRT-PCR validation  
906 of *STING* mRNA after exposure to *Flavobacterium* or *P. aeruginosa* conditioned media  
907 for three hours, compared to vehicle control. Error bars represent SD. Statistical  
908 analysis (t-test) was performed in GraphPad software **(C)** To validate the *M. brevicollis*  
909 *STING* antibody, cell lysates from *M. brevicollis* were immunoblotted alongside cell  
910 lysates from *S. rosetta*, a closely-related choanoflagellate species that does not have a  
911 *STING* homolog. A band at 36kD, the predicted size of *M. brevicollis* *STING*, is  
912 detectable in *M. brevicollis* lysate but not *S. rosetta* lysate. Arrow indicates *STING* band.  
913 Non-specific bands are likely due to co-cultured feeding bacteria. Tubulin is shown as  
914 loading control. **(D)** Protein sequence alignment (generated by Clustal Omega multiple  
915 sequence alignment) of *M. brevicollis* and animal *STING* proteins, colored by similarity.  
916 *M. brevicollis* *STING* and human *STING* are 19.1% identical and 36.6% similar at the  
917 amino acid level.

918  
919  
920

921 **Figure 3. 2'3' cGAMP, but not bacterially-produced cyclic dinucleotides, induces**  
922 **elevated levels of STING**

923 **(A)** Schematic of choanoflagellate (*M. brevicollis*), sea anemone (*N. vectensis*), insect  
924 (*D. melanogaster*) and mammalian (*M. musculus* and *H. sapiens*) *STING* proteins.  
925 Transmembrane (TM) domains are depicted in gray, *STING* cyclic dinucleotide binding  
926 domain (CDN) in purple, and C-terminal tail domain (CTT) in blue. **(B)** Partial protein  
927 sequence alignment (generated by Clustal Omega multiple sequence alignment) of *M.*  
928 *brevicollis* and animal *STING* proteins, colored by similarity. *M. brevicollis* *STING* and  
929 human *STING* are 19.1% identical and 36.6% similar at the amino acid level. Key cyclic  
930 dinucleotide-interacting residues from human *STING* structure are indicated by circles.  
931 **(C)** Dose-response curves of *M. brevicollis* exposed to cyclic dinucleotides for 24 hours  
932 reveal that treatment with 2'3'cGAMP, but not 3'3' cGAMP, c-di-AMP, or c-di-GMP,  
933 leads to *M. brevicollis* cell death in a dose-dependent manner. Data represent mean +/-  
934 SD for at least three biological replicates. **(D)** *STING* protein levels increase after

935 exposure to 2'3'cGAMP, but not bacterially-produced cyclic dinucleotides. *M. brevicollis*  
936 STING levels were examined by immunoblotting 5 hours after exposure to 2'3'cGAMP  
937 (100  $\mu$ M), 3'3'cGAMP (200  $\mu$ M), c-di-GMP (200  $\mu$ M), or c-di-AMP (200  $\mu$ M). Tubulin is  
938 shown as loading control, and intensity of STING protein bands were quantified relative  
939 to tubulin. Shown is a representative blot from three biological replicates. Statistical  
940 analysis (one-way ANOVA, Dunnett's multiple comparison) was performed in GraphPad  
941 software. **(E)** STING protein levels increase and remain elevated after exposure to 100  
942  $\mu$ M 2'3'cGAMP. Tubulin is shown as loading control, and data are representative of  
943 three biological replicates. Statistical analysis (one-way ANOVA, Dunnett's multiple  
944 comparison) was performed in GraphPad software, and *p*-values shown are calculated  
945 using 0 hour timepoint as control group.

946

947

948

949 **Figure 3 – figure supplement 1. *M. brevicollis* has distinct responses to 2'3'**  
950 **cGAMP and 3'3' cGAMP**

951 **(A,B)** Volcano plots displaying RNA-seq differential expression analysis of *M. brevicollis*  
952 treated with (A) 100  $\mu$ M 2'3'cGAMP or (B) 200  $\mu$ M 3'3'cGAMP for 3 hours, relative to an  
953 untreated control. Genes with a fold change  $\geq 2$  and false discovery rate  $\leq 10e^{-4}$  are  
954 depicted by black dots. STING is highlighted in red. RNA-seq libraries were prepared  
955 from three (2'3' cGAMP) or two (3'3' cGAMP) biological replicates. **(C)** *M. brevicollis*  
956 *STING* mRNA levels increase in response to 2'3'cGAMP. (Left) RNA-seq fold change of  
957 *STING* mRNA after exposure to 100  $\mu$ M 2'3'cGAMP or 200  $\mu$ M 3'3'cGAMP for three  
958 hours, compared to vehicle control. (Right) qRT-PCR fold change of *STING* mRNA after  
959 exposure to 100  $\mu$ M 2'3'cGAMP or 200  $\mu$ M 3'3'cGAMP for three hours, compared to  
960 vehicle control. **(D)** Venn diagram comparing the overlap of genes identified as  
961 differentially expressed after treatment with 2'3'cGAMP, 3'3'cGAMP, and *P. aeruginosa*  
962 (DEG cutoff: fold change  $\geq 3$ , false discovery rate  $\leq 10e^{-4}$ ). **(E,F)** Representative  
963 immunostained *M. brevicollis* demonstrating 2'3'cGAMP stimulates the formation of  
964 STING puncta at perinuclear regions. *M. brevicollis* was left untreated (E), or exposed to  
965 100  $\mu$ M 2'3'cGAMP (F) for 5 hours. Cells were fixed and STING levels and localization  
966 were probed using an anti-STING antibody. **(E',F')** Exposure to 2'3'cGAMP results in  
967 increased numbers of STING puncta compared to untreated controls. **(E'',F'')** Z-slice  
968 images of the plane containing the nucleus 'n' show that STING puncta localize to  
969 perinuclear regions. Green: anti-tubulin antibody (flagella and cell body), magenta: anti-  
970 STING antibody, blue: Hoechst. Scale bar represents 2  $\mu$ m.

971

972

973

974 **Figure 4. Transfection reveals STING localization to perinuclear and endoplasmic**  
975 **reticulum regions**

976 **(A)** STING-mTFP localizes to tubule-like structures around the nucleus in cells stably  
977 expressing STING-mTFP. Green: anti-tubulin antibody (flagella and cell body),  
978 magenta: anti-STING antibody, blue: Hoechst. Scale bar represents 2  $\mu\text{m}$ . **(B,C)**  
979 Fluorescent markers and live cell imaging reveal that STING is localized to the  
980 endoplasmic reticulum (ER). Cells were co-transfected with STING-mTFP and an  
981 mCherry fusion protein that localizes either to the endoplasmic reticulum (B; mCherry-  
982 HDEL) or mitochondria (C; Cox4-mCherry)<sup>4</sup>. Cells were recovered in the presence of  
983 *Flavobacterium* feeding bacteria for 28 hours after co-transfection, and then live cells  
984 were visualized with super-resolution microscopy. Each panel shows Z-slice images of  
985 a single representative cell. In confocal Z-slice images, cells are oriented with the apical  
986 flagella pointing up, and the nucleus is marked by 'n' when clearly included in the plane  
987 of focus. STING colocalized with the ER marker (B''), but not the mitochondrial marker  
988 (C''). Scale bar represents 2  $\mu\text{m}$ .

989

990

991

992 **Figure 5. STING mediates responses to 2'3'cGAMP and *P. aeruginosa***

993 **(A)** The genotypes of wild type and genome-edited *STING*<sup>-</sup> strains at the *STING* locus.  
994 **(B)** STING protein is not detectable by immunoblot in *STING*<sup>-</sup> cells. Shown is a  
995 representative blot from three biological replicates. **(C,D)** STING is necessary for  
996 2'3'cGAMP-induced cell death. **(C)** Wild type and *STING*<sup>-</sup> strains were treated with  
997 increasing concentrations of 2'3'cGAMP, and survival was quantified after 24 hours. In  
998 contrast to wild type cells, 2'3'cGAMP does not induce cell death in *STING*<sup>-</sup> cells. Data  
999 represent mean +/- SD for four biological replicates. **(D)** Wild type and *STING*<sup>-</sup> cells  
1000 were transfected with STING-mTFP, and treated with puromycin to generate stable  
1001 clonal strains. Stable expression of STING-mTFP in *STING*<sup>-</sup> cells partially rescued the  
1002 phenotype of 2'3'cGAMP-induced cell death. Data represent mean +/- SD for three  
1003 biological replicates. Statistical analysis (multiple unpaired t-tests) was performed in  
1004 GraphPad software. **(E)** Wild type and *STING*<sup>-</sup> strains have distinct transcriptional  
1005 responses to 2'3' cGAMP. Differential expression analysis was performed on wild type  
1006 and *STING*<sup>-</sup> cells treated with 100 $\mu\text{M}$  2'3'cGAMP or a vehicle control for three hours. A  
1007 heatmap comparing the log<sub>2</sub> fold change of genes identified as differentially expressed  
1008 (FC  $\geq 2$ ; FDR  $\leq 10^{-4}$ ) in wild type cells after 2'3' cGAMP treatment, to their log<sub>2</sub> fold  
1009 change in *STING*<sup>-</sup> cells after 2'3' cGAMP treatment. RNA-seq libraries were prepared  
1010 from two biological replicates. **(F)** Presence of STING in the transcriptomes of diverse  
1011 choanoflagellate species. Data from Richter et al. 2018<sup>3</sup>. **(G)** Effects of 2'3'cGAMP on  
1012 different choanoflagellate species. Choanoflagellates were grown to late-log phase, and  
1013 treated with increasing concentrations of 2'3'cGAMP. Survival was quantified after 24

1014 hours. 2'3'cGAMP only affected the survival of *M. brevicollis* and *S. macrocollata*, the  
1015 two sequenced choanoflagellate species with a STING homolog. Data represent mean  
1016 +/- SD for three biological replicates. **(H)** Wild type and *STING*<sup>-</sup> cells have similar  
1017 survival responses to LPS, suggesting that STING is not required for mediating a  
1018 response to LPS. Wild type and *STING*<sup>-</sup> strains were treated with increasing  
1019 concentrations of *E. coli* LPS, and survival was quantified after 24 hours. Data represent  
1020 mean +/- SD for four biological replicates. Statistical analysis (multiple unpaired t-tests)  
1021 was performed in GraphPad software. **(I,J)** STING renders *M. brevicollis* more  
1022 susceptible to *P. aeruginosa*-induced growth inhibition. **(I)** Wild type and *STING*<sup>-</sup> cells  
1023 were exposed to control *Flavobacterium* or *P. aeruginosa* conditioned medium (5%  
1024 vol/vol), and cell densities were quantified at indicated time points. Data represent mean  
1025 +/- SD for three biological replicates. **(J)** Percent survival calculated from growth curves  
1026 in (I). Statistical analysis (multiple unpaired t-tests) was performed in GraphPad  
1027 software.

1028  
1029  
1030

1031 **Figure 5- figure supplement 1. Characterizing *STING*<sup>-</sup> *M. brevicollis***

1032 **(A)** Sanger sequences of the consensus genotype at the site of gene editing in wild type  
1033 and *STING*<sup>-</sup> cells. *STING*<sup>-</sup> cells have a 7 base-pair deletion that leads to premature stop  
1034 codons. **(B)** Growth curves of wild type and *STING*<sup>-</sup> cells indicate that both strains have  
1035 similar growth dynamics. Statistical analysis (multiple unpaired t-tests) was performed in  
1036 GraphPad software. **(C)** Volcano plot displaying RNA-seq differential expression  
1037 analysis of *STING*<sup>-</sup> cells treated with 100 μM 2'3'cGAMP for 3 hours, relative to an  
1038 untreated control. Genes with a fold change ≥2 and false discovery rate ≤10e<sup>-4</sup> are  
1039 depicted by black dots. RNA-seq libraries were prepared from two biological replicates.  
1040 **(D)** Venn diagram comparing the overlap of genes identified as differentially expressed  
1041 (FC ≥3; FDR ≤10<sup>-4</sup>) after treatment with 2'3'cGAMP in wild type and *STING*<sup>-</sup> cells. **(E)**  
1042 Protein sequence alignment (generated by Clustal Omega multiple sequence  
1043 alignment) of STING proteins from choanoflagellates *S. macrocollata* and *M. brevicollis*  
1044 and animals, colored by similarity.

1045  
1046  
1047

1048 **Figure 6. STING mediates 2'3'cGAMP-induced autophagic pathway**

1049 **(A)** 2'3'cGAMP-induced Atg8 lipidation requires STING. WT and *STING*<sup>-</sup> cells stably  
1050 expressing mCherry-Atg8 were treated with a vehicle control or 100 μM 2'3'cGAMP for  
1051 3 hours, followed by immunoblotting. The band intensity of Atg8-I (unmodified Atg8) and  
1052 Atg8-II (lipidated Atg8) were quantified for each sample. Relative levels of Atg8  
1053 lipidation were assessed by dividing the band intensities of Atg8-II/Atg8-I. Tubulin is

1054 shown as loading control. Immunoblot is representative of three biological replicates.  
1055 **(B)** 2'3'cGAMP induces Atg8 lipidation in chloroquine-treated wild type cells. WT cells  
1056 stably expressing mCherry-Atg8 were first incubated with 40 mM chloroquine for 6  
1057 hours, and then treated with a vehicle control or 100  $\mu$ M 2'3'cGAMP for 3 hours in the  
1058 presence of chloroquine, followed by immunoblotting. For each sample, relative levels  
1059 of Atg8 lipidation were assessed by dividing the band intensities of Atg8-II/Atg8-I.  
1060 Tubulin is shown as loading control. Immunoblot is representative of three biological  
1061 replicates. For a representative immunoblot and quantification of Atg8-II/Atg8-I levels in  
1062 chloroquine-treated *STING*<sup>-</sup> cells, refer to Figure 6 - figure supplement 1B. **(C-G)**  
1063 STING is required for 2'3'cGAMP-induced autophagosome formation. **(C-F)** WT and  
1064 *STING*<sup>-</sup> cells stably expressing mCherry-Atg8 were treated with a vehicle control or 100  
1065  $\mu$ M 2'3'cGAMP for 3 hours, and then fixed and immunostained. **(C,D)** Representative  
1066 confocal images of wild type cells show that Atg8 puncta accumulate after 2'3'cGAMP  
1067 treatment. Magenta: mCherry-Atg8; Green: anti-tubulin antibody (flagella and cell body).  
1068 **(E,F)** Representative confocal images of *STING*<sup>-</sup> cells show that Atg8 remains evenly  
1069 distributed in the cytoplasm after 2'3'cGAMP treatment. **(G)** The number of Atg8  
1070 puncta/cell was quantified for WT and *STING*<sup>-</sup> cells treated with a vehicle control or  
1071 2'3'cGAMP for three hours. Data represent cells quantified from two biological replicates  
1072 (n=150 cells per treatment group). Statistical analyses (unpaired two-tailed t-tests) were  
1073 performed in GraphPad software. **(H)** Treatment with lysosomotropic agents that inhibit  
1074 autophagy rescue 2'3' cGAMP-induced cell death in wild type cells. WT and *STING*<sup>-</sup>  
1075 cells were pre-treated with 40 mM chloroquine, 10mM NH<sub>4</sub>Cl, or a vehicle control for 6  
1076 hours. Cells were then exposed to either 100  $\mu$ M 2'3'cGAMP or a vehicle control for 18  
1077 hours before quantifying survival. Data represent mean +/- SD for three biological  
1078 replicates. Statistical analyses (multiple unpaired t-tests) were performed in GraphPad  
1079 software.

1080  
1081

1082 **Figure 6 – figure supplement 1. STING mediates 2'3'cGAMP-induced autophagic**  
1083 **signaling**

1084 **(A)** Overexpression of mCherry-Atg8 does not alter the susceptibility of wild type and  
1085 *STING*<sup>-</sup> strains to 2'3'cGAMP. Wild type and *STING*<sup>-</sup> strains stably expressing mCherry-  
1086 Atg8 were treated with increasing concentrations of 2'3'cGAMP, and survival was  
1087 quantified after 24 hours. Data represent mean +/- SD for two biological replicates. **(B)**  
1088 2'3'cGAMP does not induce increased Atg8 lipidation in chloroquine-treated *STING*<sup>-</sup>  
1089 cells. *STING*<sup>-</sup> cells stably expressing mCherry-Atg8 were incubated with 40 mM  
1090 chloroquine for 6 hours, and then treated with a vehicle control or 100  $\mu$ M 2'3'cGAMP  
1091 for 3 hours in the presence of chloroquine, followed by immunoblotting. For each  
1092 sample, relative levels of Atg8 lipidation were assessed by dividing the band intensities  
1093 of Atg8-II/Atg8-I. Tubulin is shown as loading control. Immunoblot is representative of

1094 three biological replicates. Statistical analyses (unpaired two-tailed t-tests) were  
1095 performed in GraphPad software.

1096

1097 **Source data file 1.** Uncropped western blots for: Figure 2- figure supplement 1C,  
1098 Figure 2C, Figure 3D, Figure 3E, Figure 5B, Figure 6A, Figure 6B, Figure 6-  
1099 supplement1B



## **References**

1. Shabalina, S. A. & Koonin, E. V. Origins and evolution of eukaryotic RNA interference. *Trends Ecol Evol* **23**, 578–587 (2008).
2. Richter, D. J. & Levin, T. C. The origin and evolution of cell-intrinsic antibacterial defenses in eukaryotes. *Curr Opin Genet Dev* **58–59**, 111–122 (2019).
3. Richter, D. J., Fozouni, P., Eisen, M. B. & King, N. Gene family innovation, conservation and loss on the animal stem lineage. *Elife* **7**, 946 (2018).
4. King, N. *et al.* The genome of the choanoflagellate *Monosiga brevicollis* and the origin of metazoans. *Nature* **451**, 783–788 (2008).
5. Brunet, T. & King, N. The Origin of Animal Multicellularity and Cell Differentiation. *Dev Cell* **43**, 124–140 (2017).
6. Richter, D. J. & King, N. The genomic and cellular foundations of animal origins. *Annu Rev Genet* **47**, 509–537 (2013).
7. Leadbeater, B. S. C. *The Choanoflagellates: Evolution, Ecology, and Biology*. (Cambridge University Press, 2015).
8. Dayel, M. J. & King, N. Prey capture and phagocytosis in the choanoflagellate *Salpingoeca rosetta*. *Plos One* **9**, e95577 (2014).
9. Wu, X. *et al.* Molecular evolutionary and structural analysis of the cytosolic DNA sensor cGAS and STING. *Nucleic Acids Res* **42**, 8243–8257 (2014).
10. Levin, T. C., Greaney, A. J., Wetzel, L. & King, N. The Rosetteless gene controls development in the choanoflagellate *S. rosetta*. *Elife* **3**, (2014).
11. Ablasser, A. & Chen, Z. J. cGAS in action: Expanding roles in immunity and inflammation. *Science* **363**, eaat8657 (2019).
12. Ahn, J. & Barber, G. N. STING signaling and host defense against microbial infection. *Exp Mol Medicine* **51**, 1–10 (2019).
13. Margolis, S. R., Wilson, S. C. & Vance, R. E. Evolutionary Origins of cGAS-STING Signaling. *Trends Immunol* **38**, 733–743 (2017).
14. Kranzusch, P. J. *et al.* Ancient Origin of cGAS-STING Reveals Mechanism of Universal 2',3' cGAMP Signaling. *Mol Cell* **59**, 891–903 (2015).
15. Ishikawa, H. & Barber, G. N. STING is an endoplasmic reticulum adaptor that facilitates innate immune signalling. *Nature* **455**, 674–678 (2008).

16. Sun, L., Wu, J., Du, F., Chen, X. & Chen, Z. J. Cyclic GMP-AMP Synthase Is a Cytosolic DNA Sensor That Activates the Type I Interferon Pathway. *Science* **339**, 786–791 (2013).
17. Burdette, D. L. *et al.* STING is a direct innate immune sensor of cyclic di-GMP. *Nature* **478**, 515–518 (2011).
18. Diner, E. J. *et al.* The Innate Immune DNA Sensor cGAS Produces a Noncanonical Cyclic Dinucleotide that Activates Human STING. *Cell Reports* **3**, 1355–1361 (2013).
19. Gao, P. *et al.* Cyclic [G(2',5')pA(3',5')p] Is the Metazoan Second Messenger Produced by DNA-Activated Cyclic GMP-AMP Synthase. *Cell* **153**, 1094–1107 (2013).
20. Ablasser, A. *et al.* cGAS produces a 2'-5'-linked cyclic dinucleotide second messenger that activates STING. *Nature* **498**, 380–384 (2013).
21. Moretti, J. *et al.* STING Senses Microbial Viability to Orchestrate Stress-Mediated Autophagy of the Endoplasmic Reticulum. *Cell* **171**, 809-823.e13 (2017).
22. Cohen, D. *et al.* Cyclic GMP-AMP signalling protects bacteria against viral infection. *Nature* **574**, 691–695 (2019).
23. Morehouse, B. R. *et al.* STING cyclic dinucleotide sensing originated in bacteria. *Nature* 1–8 (2020) doi:10.1038/s41586-020-2719-5.
24. Burroughs, A. M. & Aravind, L. Identification of Uncharacterized Components of Prokaryotic Immune Systems and Their Diverse Eukaryotic Reformulations. *J Bacteriol* **202**, (2020).
25. Alegado, R. A. *et al.* A bacterial sulfonolipid triggers multicellular development in the closest living relatives of animals. *Elife* **1**, e00013 (2012).
26. Brunet, T. *et al.* A flagellate-to-amoeboid switch in the closest living relatives of animals. *Elife* **10**, e61037 (2021).
27. Dayel, M. J. *et al.* Cell differentiation and morphogenesis in the colony-forming choanoflagellate *Salpingoeca rosetta*. *Dev Biol* **357**, 73–82 (2011).
28. Woznica, A., Gerdt, J. P., Hulett, R. E., Clardy, J. & King, N. Mating in the Closest Living Relatives of Animals Is Induced by a Bacterial Chondroitinase. *Cell* **170**, 1175–1183.e11 (2017).
29. Brunet, T. *et al.* Light-regulated collective contractility in a multicellular choanoflagellate. *Science* **366**, 326–334 (2019).
30. Laundon, D., Larson, B. T., McDonald, K., King, N. & Burkhardt, P. The architecture of cell differentiation in choanoflagellates and sponge choanocytes. *Plos Biol* **17**, e3000226 (2019).

31. Woznica, A. *et al.* Bacterial lipids activate, synergize, and inhibit a developmental switch in choanoflagellates. *Proc National Acad Sci* **113**, 7894–7899 (2016).
32. Ireland, E. V., Woznica, A. & King, N. Synergistic Cues from Diverse Bacteria Enhance Multicellular Development in a Choanoflagellate. *Appl Environ Microb* **86**, (2020).
33. Hake, K. *et al.* Colonial choanoflagellate isolated from Mono Lake harbors a microbiome. doi:10.1101/2021.03.30.437421.
34. Moradali, M. F., Ghods, S. & Rehm, B. H. A. *Pseudomonas aeruginosa* Lifestyle: A Paradigm for Adaptation, Survival, and Persistence. *Front Cell Infect Mi* **7**, 39 (2017).
35. Mahajan-Miklos, S., Tan, M.-W., Rahme, L. G. & Ausubel, F. M. Molecular Mechanisms of Bacterial Virulence Elucidated Using a *Pseudomonas aeruginosa*–*Caenorhabditis elegans* Pathogenesis Model. *Cell* **96**, 47–56 (1999).
36. Pukatzki, S., Kessin, R. H. & Mekalanos, J. J. The human pathogen *Pseudomonas aeruginosa* utilizes conserved virulence pathways to infect the social amoeba *Dictyostelium discoideum*. *Proc National Acad Sci* **99**, 3159–3164 (2002).
37. Rahme, L. G. *et al.* Use of model plant hosts to identify *Pseudomonas aeruginosa* virulence factors. *Proc National Acad Sci* **94**, 13245–13250 (1997).
38. Uribe-Querol, E. & Rosales, C. Control of Phagocytosis by Microbial Pathogens. *Front Immunol* **8**, 1368 (2017).
39. Yoon, S. *et al.* *Pseudomonas syringae* evades phagocytosis by animal cells via type III effector-mediated regulation of actin filament plasticity. *Environ Microbiol* **20**, 3980–3991 (2018).
40. Klockgether, J. & Tümmler, B. Recent advances in understanding *Pseudomonas aeruginosa* as a pathogen. *F1000research* **6**, 1261 (2017).
41. Tanaka, Y. & Chen, Z. J. STING Specifies IRF3 Phosphorylation by TBK1 in the Cytosolic DNA Signaling Pathway. *Sci Signal* **5**, ra20–ra20 (2012).
42. Liu, S. *et al.* Phosphorylation of innate immune adaptor proteins MAVS, STING, and TRIF induces IRF3 activation. *Science* **347**, aaa2630 (2015).
43. Zhang, C. *et al.* Structural basis of STING binding with and phosphorylation by TBK1. *Nature* **567**, 394–398 (2019).
44. Abe, T. & Barber, G. N. Cytosolic-DNA-Mediated, STING-Dependent Proinflammatory Gene Induction Necessitates Canonical NF- $\kappa$ B Activation through TBK1. *J Virol* **88**, 5328–5341 (2014).

45. Gui, X. *et al.* Autophagy induction via STING trafficking is a primordial function of the cGAS pathway. *Nature* **567**, 262–266 (2019).
46. Yamashiro, L. H. *et al.* Interferon-independent STING signaling promotes resistance to HSV-1 in vivo. *Nat Commun* **11**, 3382 (2020).
47. Prabakaran, T. *et al.* Attenuation of cGAS-STING signaling is mediated by a p62/SQSTM1-dependent autophagy pathway activated by TBK1. *Embo J* **37**, (2018).
48. Mann, C. C. de O. *et al.* Modular Architecture of the STING C-Terminal Tail Allows Interferon and NF- $\kappa$ B Signaling Adaptation. *Cell Reports* **27**, 1165-1175.e5 (2019).
49. Watson, R. O. *et al.* The Cytosolic Sensor cGAS Detects Mycobacterium tuberculosis DNA to Induce Type I Interferons and Activate Autophagy. *Cell Host Microbe* **17**, 811–819 (2015).
50. Booth, D. S., Szmidt-Middleton, H. & King, N. Choanoflagellate transfection illuminates their cell biology and the ancestry of animal septins. *Mol Biol Cell* **29**, mbcE18080514 (2018).
51. Dobbs, N. *et al.* STING Activation by Translocation from the ER Is Associated with Infection and Autoinflammatory Disease. *Cell Host Microbe* **18**, 157–168 (2015).
52. Booth, D. S. & King, N. Genome editing enables reverse genetics of multicellular development in the choanoflagellate *Salpingoeca rosetta*. *Elife* **9**, e56193 (2020).
53. Liu, Y. *et al.* Inflammation-Induced, STING-Dependent Autophagy Restricts Zika Virus Infection in the Drosophila Brain. *Cell Host Microbe* **24**, 57-68.e3 (2018).
54. Klionsky, D. J. *et al.* Guidelines for the use and interpretation of assays for monitoring autophagy (4th edition) 1. *Autophagy* **17**, 1–382 (2021).
55. Tanida, I., Minematsu-Ikeguchi, N., Ueno, T. & Kominami, E. Lysosomal Turnover, but Not a Cellular Level, of Endogenous LC3 is a Marker for Autophagy. *Autophagy* **1**, 84–91 (2005).
56. Pokatayev, V. *et al.* Homeostatic regulation of STING protein at the resting state by stabilizer TOLLIP. *Nat Immunol* **21**, 158–167 (2020).
57. McFarland, A. P. *et al.* Sensing of Bacterial Cyclic Dinucleotides by the Oxidoreductase RECON Promotes NF- $\kappa$ B Activation and Shapes a Proinflammatory Antibacterial State. *Immunity* **46**, 433–445 (2017).
58. Margolis, S. R. *et al.* The STING ligand 2'3'-cGAMP induces an NF- $\kappa$ B-dependent anti-bacterial innate immune response in the starlet sea anemone *Nematostella vectensis*. (2021) doi:10.1101/2021.05.13.443009.
59. Cai, H. *et al.* 2'3'-cGAMP triggers a STING- and NF- $\kappa$ B-dependent broad antiviral response in Drosophila. *Sci Signal* **13**, eabc4537 (2020).

60. Martin, M., Hiroyasu, A., Guzman, R. M., Roberts, S. A. & Goodman, A. G. Analysis of *Drosophila* STING Reveals an Evolutionarily Conserved Antimicrobial Function. *Cell Reports* **23**, 3537-3550.e6 (2018).
61. Goto, A. *et al.* The Kinase IKK $\beta$  Regulates a STING- and NF- $\kappa$ B-Dependent Antiviral Response Pathway in *Drosophila*. *Immunity* **49**, 225-234.e4 (2018).
62. Hua, X. *et al.* Stimulator of interferon genes (STING) provides insect antiviral immunity by promoting Dredd caspase-mediated NF- $\kappa$ B activation. *J Biol Chem* **293**, 11878–11890 (2018).
63. Schindelin, J. *et al.* Fiji: an open-source platform for biological-image analysis. *Nat Methods* **9**, 676–682 (2012).
64. Kim, D. *et al.* TopHat2: accurate alignment of transcriptomes in the presence of insertions, deletions and gene fusions. *Genome Biol* **14**, R36 (2013).
65. Liao, Y., Smyth, G. K. & Shi, W. featureCounts: an efficient general purpose program for assigning sequence reads to genomic features. *Bioinformatics* **30**, 923–930 (2014).
66. Robinson, M. D., McCarthy, D. J. & Smyth, G. K. edgeR: a Bioconductor package for differential expression analysis of digital gene expression data. *Bioinformatics* **26**, 139–140 (2010).
67. Peng, D., Kurup, S. P., Yao, P. Y., Minning, T. A. & Tarleton, R. L. CRISPR-Cas9-Mediated Single-Gene and Gene Family Disruption in *Trypanosoma cruzi*. *Mbio* **6**, e02097-14 (2015).

**Table 1. Bacteria screened for pathogenic effects**

<b>Bacterium</b>	<b>Pathogenic effects</b>	<b>Reference or details</b>	<b>Source</b>
<i>Aeromonas hydrophila</i>	–	Environmental isolate	This study
<i>Bacillus aquimaris</i>	–	Environmental isolate	This study
<i>Bacillus badius</i>	–	Mouse isolate	Julie Pfeiffer
<i>Bacillus cereus</i>	–	Environmental isolate	This study
<i>Bacillus indicus</i>	–	Environmental isolate	This study
<i>Bacillus marisflavi</i>	–	Environmental isolate	This study
<i>Bacillus pumilus</i>	–	Mouse isolate	Julie Pfeiffer
<i>Bacillus safensis</i>	–	Mouse isolate	Julie Pfeiffer
<i>Bacillus subtilis</i>	–	ATCC 6633	Julie Pfeiffer
<i>Bacteroides acidifaciens</i>	–	Mouse isolate	Julie Pfeiffer
<i>Burkholderia multivorans</i>	–	ATCC 17616	David Greenberg
<i>Campylobacter jejuni</i> GFP	–	DRH3123	David Hendrixson
<i>Deinococcus</i> sp.	–	Environmental isolate	This study
<i>Enterococcus cloacae</i>	–	Mouse isolate	Julie Pfeiffer
<i>Enterococcus faecium</i>	–	Mouse isolate	Julie Pfeiffer
<i>Escherichia coli</i> BW25113	–	Datsenko and Wanner, 2000	David Greenberg
<i>Escherichia coli</i> DH5a GFP	–		David Hendrixson
<i>Escherichia coli</i> ECC-1470	–	Leimbach et al., 2015	Julie Pfeiffer
<i>Escherichia coli</i> K12	–	ATCC 10798	Julie Pfeiffer
<i>Flavobacterium</i> sp.	–	King et al., 2008	Isolated from ATCC PRA-258
<i>Lactobacillus johnsonii</i>	–	Mouse isolate	Julie Pfeiffer
<i>Pseudoalteromonas</i> sp.	–	Environmental isolate	This study
<i>Pseudomonas aeruginosa</i> PA-14	+	Rahm et al., 1995	Andrew Koh
<i>Pseudomonas aeruginosa</i> PAO1	+	ATCC 15692	David Greenberg
<i>Pseudomonas aeruginosa</i> PAO1-GFP	+	Bloemberg et al., 1997	David Greenberg
<i>Pseudomonas granadensis</i>	–	Environmental isolate	This study
<i>Staphylococcus aureus</i>	–	ATCC 23235	Julie Pfeiffer
<i>Staphylococcus</i> sp.	–	Mouse isolate	Julie Pfeiffer
<i>Vibrio alginolyticus</i>	–	Environmental isolate	Kim Orth
<i>Vibrio furnissii</i>	–	Environmental isolate	This study
<i>Vibrio parahaemolyticus</i>	–	Environmental isolate	This study
<i>Vibrio parahaemolyticus</i> RimD- GFP	–	Ritchie et al., 2012	Kim Orth
<i>Vibrio ruber</i>	–	Environmental isolate	This study
<i>Vibrio</i> sp.	–	Environmental isolate	This study

**Table 2. *P. aeruginosa* deletion strains**

Strain name	Gene	Putative ORF function	Effects on <i>M. brevicollis</i>	
			Truncated Flagellum/ Settling	Cell Death
MPAO1		parent to library stain	+	+
PW5035	pvdE	pyoverdine biosynthesis protein PvdE	+	+
PW5034	pvdE	pyoverdine biosynthesis protein PvdE	+	+
PW1059	exoT	exoenzyme T	+	+
PW3078	toxA	exotoxin A precursor	+	+
PW3079	toxA	exotoxin A precursor	+	+
PW4736	exoY	adenylate cyclase ExoY	+	+
PW4737	exoY	adenylate cyclase ExoY	+	+
PW6886	rhIA	rhamnosyltransferase chain A	+	+
PW6887	rhIA	rhamnosyltransferase chain A	+	+
PW7478	exoS	exoenzyme S	+	+
PW7479	exoS	exoenzyme S	+	+
PW7303	lasB	elastase LasB	+	+
PW7302	lasB	elastase LasB	+	+
PW3252	aprA	alkaline metalloproteinase precursor	+	+
PW3253	aprA	alkaline metalloproteinase precursor	+	+
PW4282	lasA	LasA protease precursor	+	+
PW4283	lasA	LasA protease precursor	+	+
RP436	popB	T3SS translocase	+	+
RP576	exoS, exoT, exoY	T3SS effector molecules	+	+

**Table 3. *M. brevicollis* response to *P. aeruginosa* factors**

<b>Treatment</b>	<b>Cell Death</b>	<b>Interpretation</b>
Live <i>P. aeruginosa</i>	++	
<i>P. aeruginosa</i> conditioned media (CM)	++	Factor(s) are secreted by <i>P. aeruginosa</i>
<i>P. aeruginosa</i> outer membrane vesicles	–	Factor(s) are not present in outer membrane vesicles
CM, boiled 20 min	++	Factor(s) are not heat labile
CM + proteinase K, followed by 80C for 30 min	++	Factor(s) are not proteins
CM + DNase and RNase	++	Factor(s) are not nucleic acids
CM MeOH extraction	++	Factor(s) are organic compounds



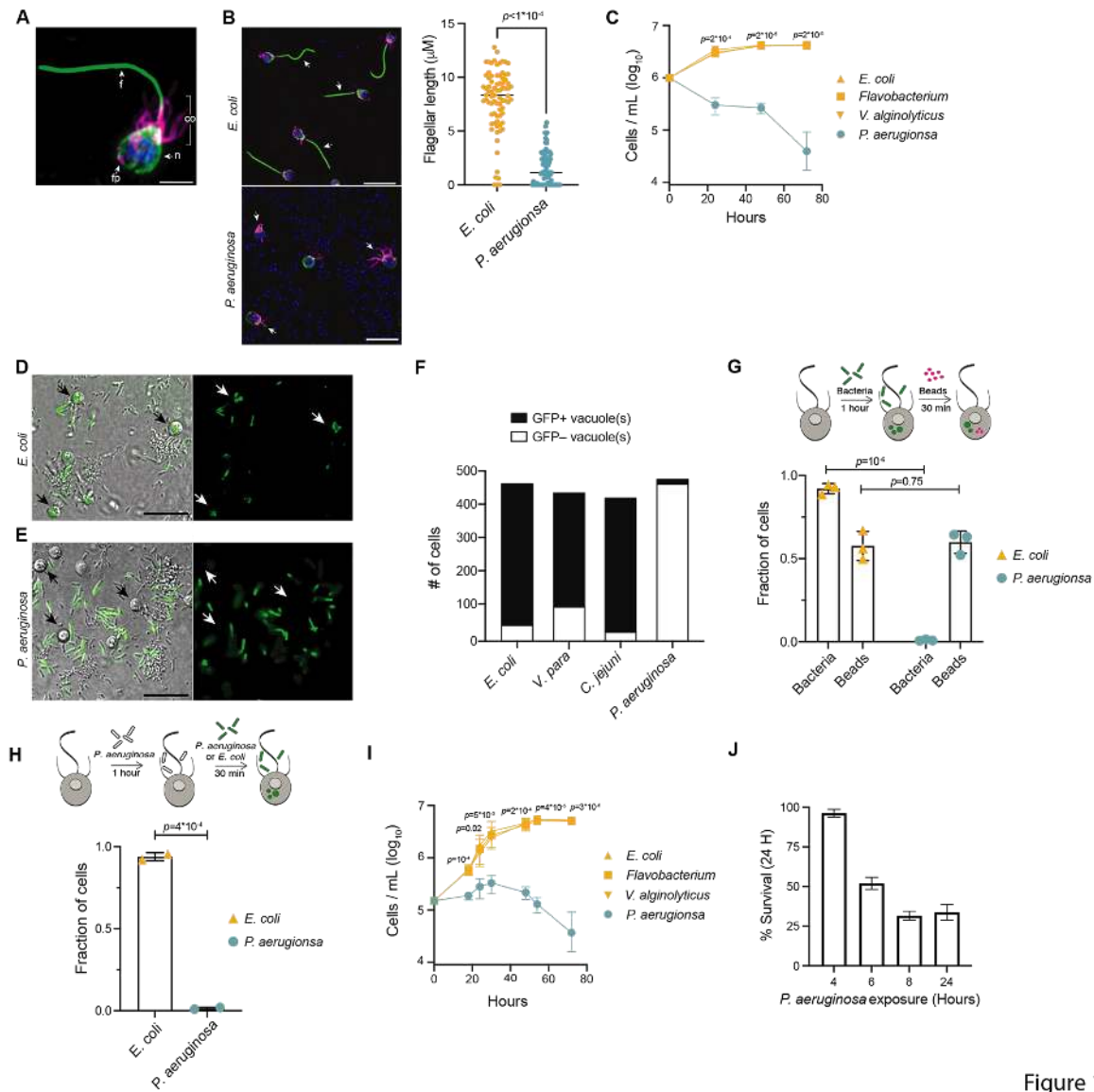


Figure 1

A

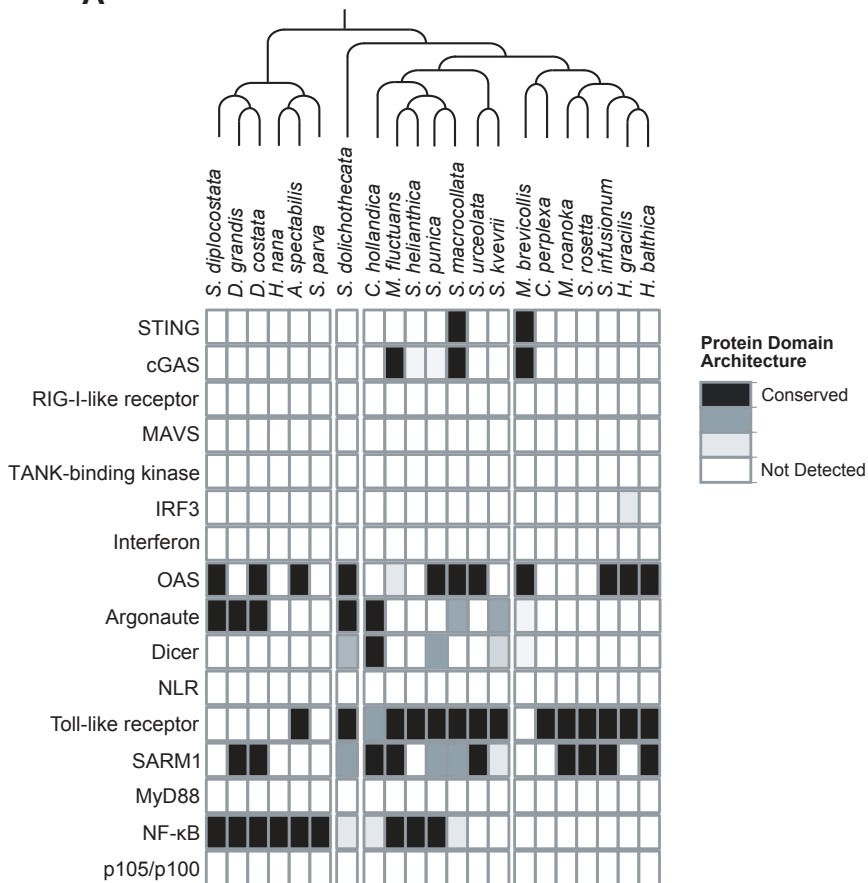


Figure 1 - figure supplement 1

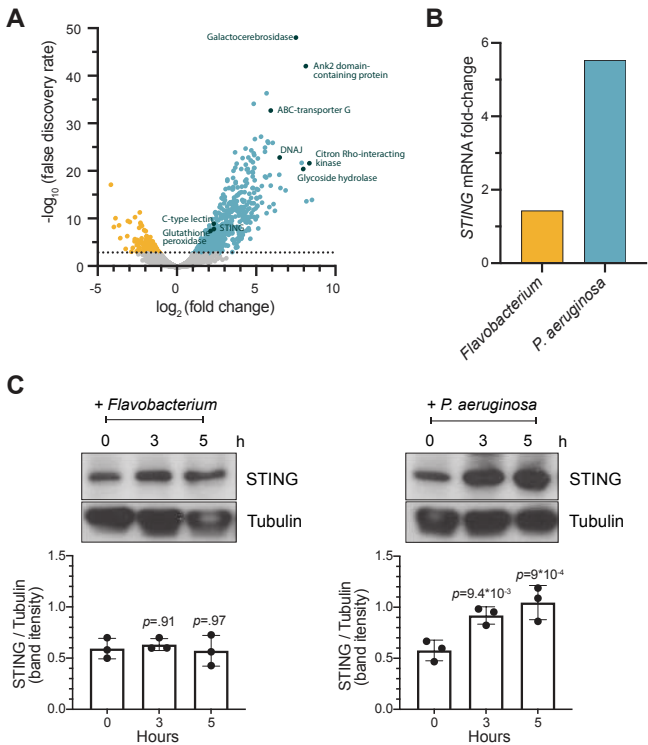
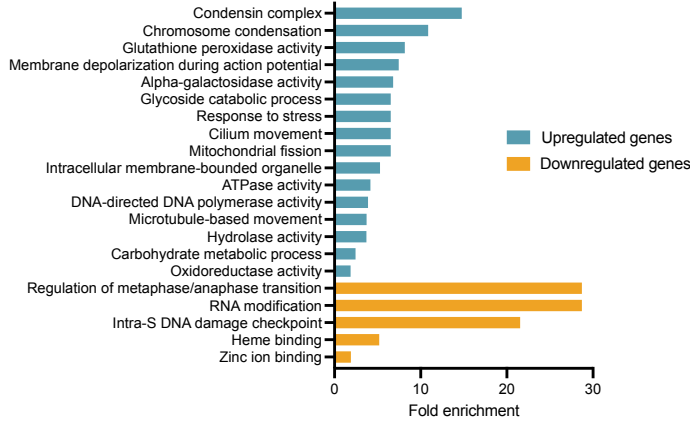
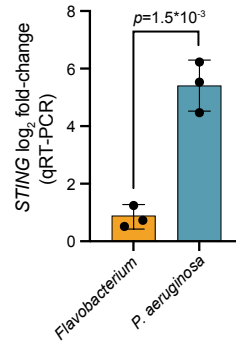


Figure 2

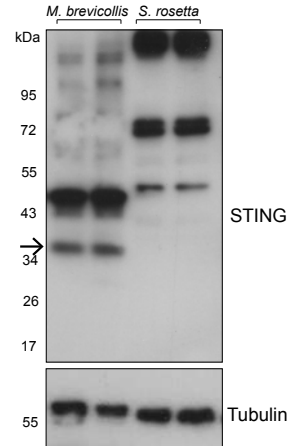
A



B



C



D

Multiple sequence alignments of STING protein domains across various species, including *M. brevicollis*, *D. melanogaster*, *N. vectensis*, *M. musculus*, and *H. sapiens*. The alignments are shown in blocks, with amino acid positions indicated on the left and right of each sequence. Conserved residues are highlighted in purple.

```

M. brevicollis  1 MM---V NLSDSLSHLSORGWAQVFVTLA-----AAAISIF 31
D. melanogaster 1 MAI--ASNVYEAGAVRAEKGRKYFYFRK-----MIGDYIDTSIRIV 40
N. vectensis   1 MRRAENNGFTPKRRNOHTPFYASIGMIVVIVAFTSYHITSYGDDRNRAMRQY 56
M. musculus    1 ---MPYSNLHPASIPRPRGHRSKYVALI-FLVASL-----MILWVAKDPPNHTLKYL 47
H. sapiens     1 ---MPHSSSLHPSSIPCPRGHGAQKAALV-LLSACL-----VTLWGLGEPPEHTLRYL 47

M. brevicollis 32 YFSFSPFEVAAGICASIAAAGAVPLLFDAVHYLIAFCISAPARP-----PLRTVW 82
D. melanogaster 41 ---ATVFLADLLRLYROVVEYGSNGRYYLPEDRLW 73
N. vectensis   57 SFTFSLA-----YLAFLVGELRRROCLFAEYRHIETRY--NGSLK 95
M. musculus    48 ---ALH-----LASHELGLLLKNLCCLAEELCHVQSRY--QGSYW 82
H. sapiens     48 ---VLH-----LASLQLGLLLNGVCSLAEELRHIHSRY--RGSYW 82

M. brevicollis 83 TKTRLQRWSGLSILTFIVLAOGLY---FASPSP-----112
D. melanogaster 74 IILLR--SCTYNNRSIYLIVGFLLVAFFRISVT--GNY-----RNVMPTTLFLFQMP 121
N. vectensis   96 KAIQTTFSFGGNNV-LFVASLFFVVFVASNDNGSSSVIQGNSTAEPHT--EMRQT 149
M. musculus    83 KAVRACLGCPIHCMAMILLSSYFYFLQNTADIY-----Y-----115
H. sapiens     83 RTVRACLGCPLRRGALLLLSIYFYYSLPNAVGPE-----P-----116

M. brevicollis 113 MSANLFAVFALSLCNSVFSAMVAPRCGRLEVVD-LATHPNTVLFRDFGAASMSYW 168
D. melanogaster 122 LYWI--WSFT-----DMDQSTLSYSHWIRDSHGLDYAAAGMASNYF 159
N. vectensis   150 SGWGLWGOFIIS-----ALLTPLVVHLLGLRELSKVEESQLNEKNKNVADGLAWSY 203
M. musculus    116 LSWM--FGL-----LVLYKSLSMLLLGLQSLTPAEVSAVCEEKKLNVAHGLAWSY 163
H. sapiens     117 FTWM--LAL-----LGLSQALNLILLGLKGLAPAEISAVCEKGNFNVAHGLAWSY 164

M. brevicollis 169 HGYLQHIAGDFAA-----LEERFRDSDVGMRVPRKLYILVPQDCEVNASDNKY 217
D. melanogaster 160 HGYLLSLPERKDDGLKHRLAMYEDKNN---VTFGIKRLVLIPDEMFVNGVLESH 212
N. vectensis   204 FGYLKFVLPELEK-----QIEKTSKFRS---KEKFVKMFLIPSNCFWDDKIPGS 251
M. musculus    164 IGYLRLILPGLQA-----RIRMFNQLHNNMLSGAGSRRLYILFPLDCGVPDNLSV 214
H. sapiens     165 IGYLRLILPGLQA-----RIRTYNQHYNNLLRGAVSQRLYILLPLDCGVPDNLSMA 215

M. brevicollis 218 E---GLKATEHYISPPKITIGGVVDREMGKHTLYTPSEESAETASVAFAMELASPLN 270
D. melanogaster 213 LLD---KAEPLETQFINRAGVY-RPFKHDVYRMNKKVNGRTYFAVEGATPMI 261
N. vectensis   252 DYDPQNRITFEGNTEPLEKTRGGVFLRRHY-KHSVYEIKDGE-NEPWFCIMEYATPLL 306
M. musculus    215 DP---NIRFRDMLPQNIDRAGIKNRVY-SNSVYEILENGQPAGVCILEYATPLO 265
H. sapiens     216 DP---NIRFLDKLPQTGDRAGIKDRVY-SNSYELLENGQRAGTCVLEYATPLO 266

M. brevicollis 271 TMKNALKDAEGLLEL-----QSEAFYLTLRGLKQEGVDQGNDEMIKLVWEK 320
D. melanogaster 262 SFFDATYSNLSGTWQMQELKREIWIKFYKHLKELITTWPET-----RDLVELIIYNS 313
N. vectensis   307 TLYDMSVAQPGELSR--EERDAOVVFLRLKLQDILEGDRAC-----QKYELVTFSP 356
M. musculus    266 TLFAMSQDAKAGFSR--EDRLEQAKLFCRTLEELEDVPES-----RNNCRLIVYQE 315
H. sapiens     267 TLFAMSQYSQAGFSR--EDRLEQAKLFCRTLEDLADAPES-----QNNCRLIAYQE 316

M. brevicollis 321 N-----RSEVLKKMFRAEDQYAMP-----338
D. melanogaster 314 HDSKGNLVDVGELLVAHMQNKTIDEISN-----343
N. vectensis   357 DRDLA-----DVMLRLKLKDSE--LEIGG-----377
M. musculus    316 PTDGNS-FSLSQEVLRHIRQEEKEEVTMNAPMTSVAPPPSVLSQEPRLLISGMDQPL 371
H. sapiens     317 PADDSSF-FSLSQEVLRHLRQEEKEEVTVGSLKTSAVPSTSTMSQEPELLISGMEKPL 372

M. brevicollis -----
D. melanogaster -----
N. vectensis -----
M. musculus 372 PLRTDLI 378
H. sapiens 373 PLRTDFS 379

```

Figure 2 - figure supplement 1

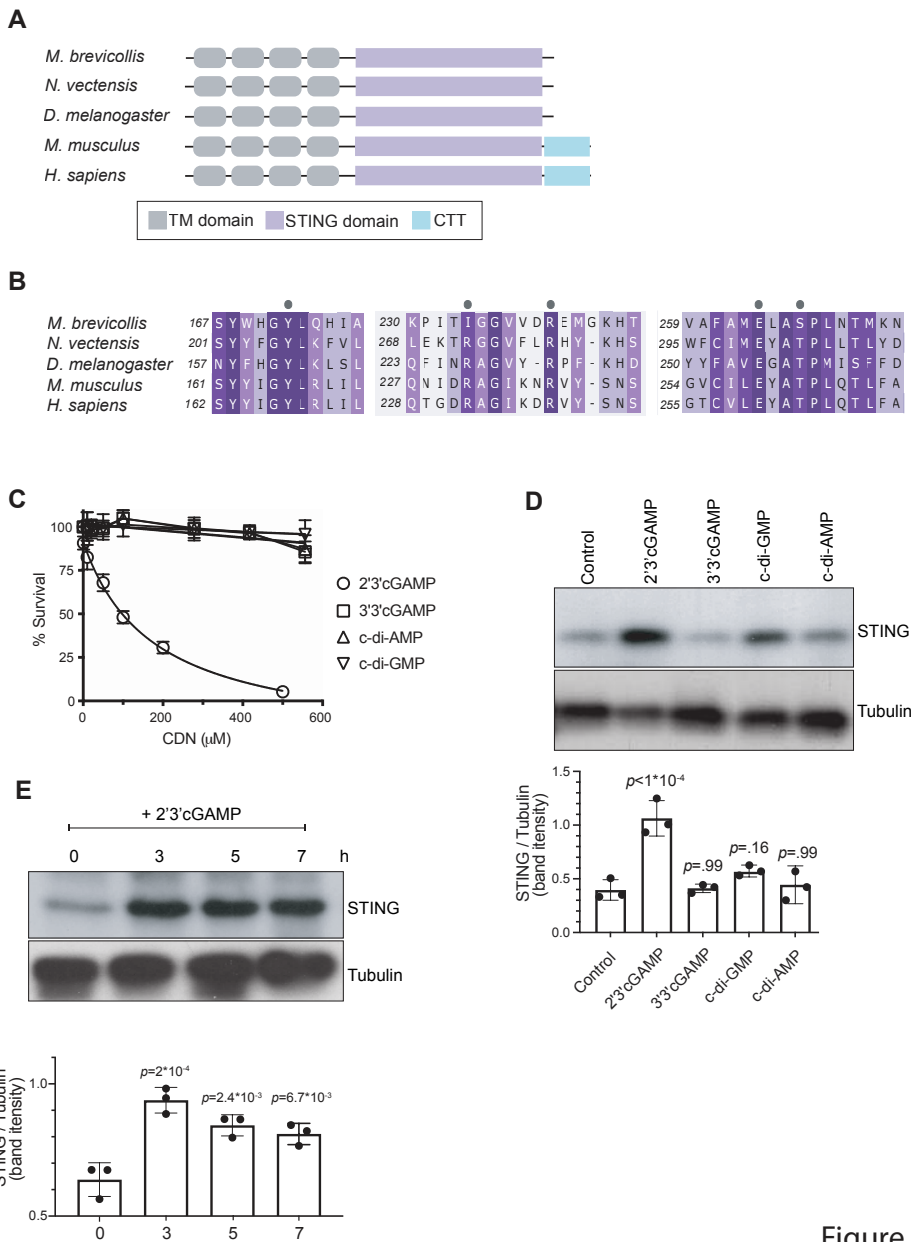


Figure 3

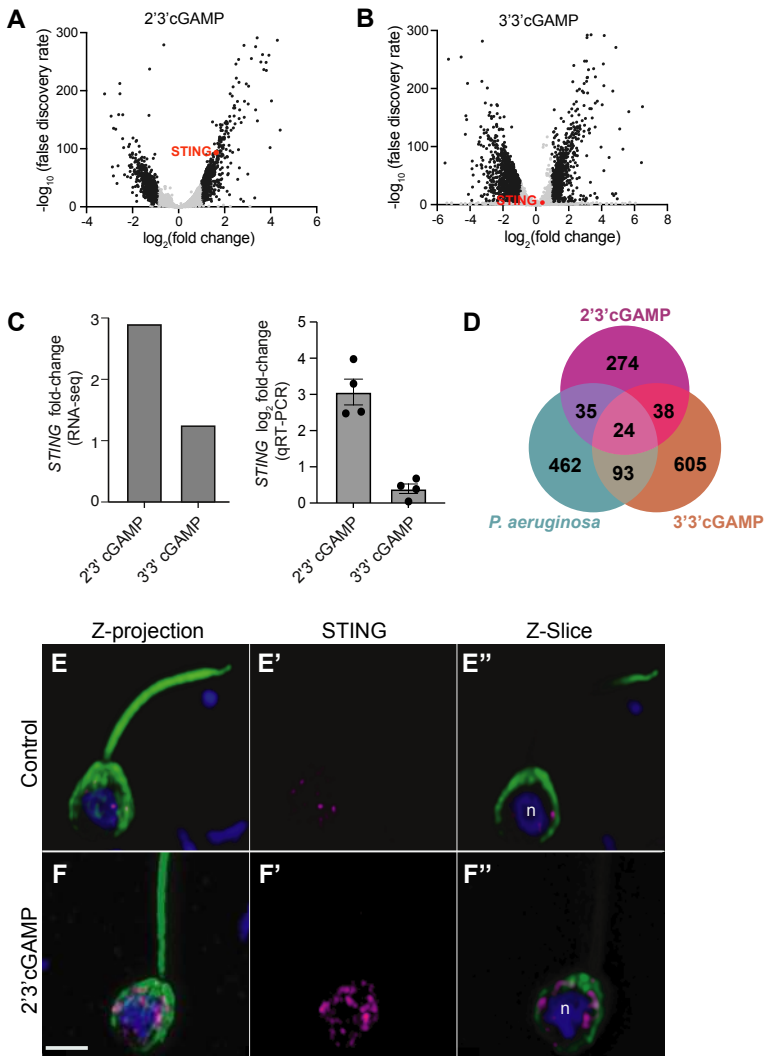


Figure 3 - figure supplement 1

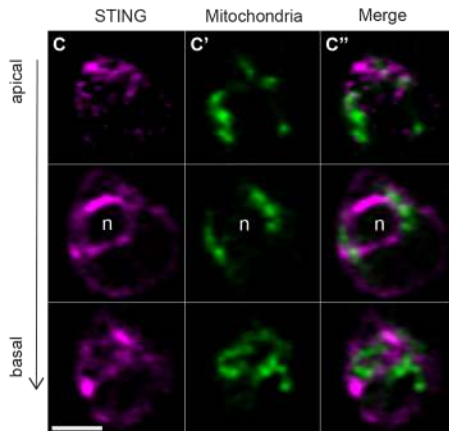
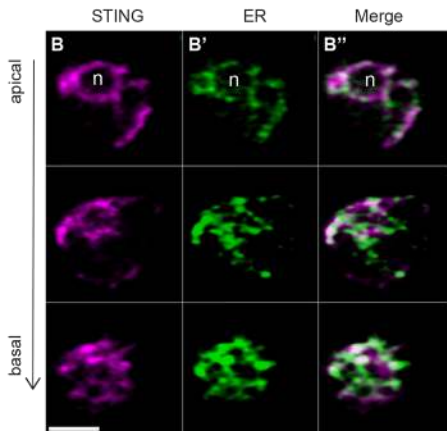
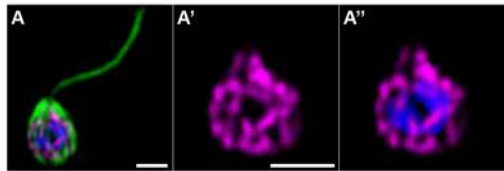


Figure 4

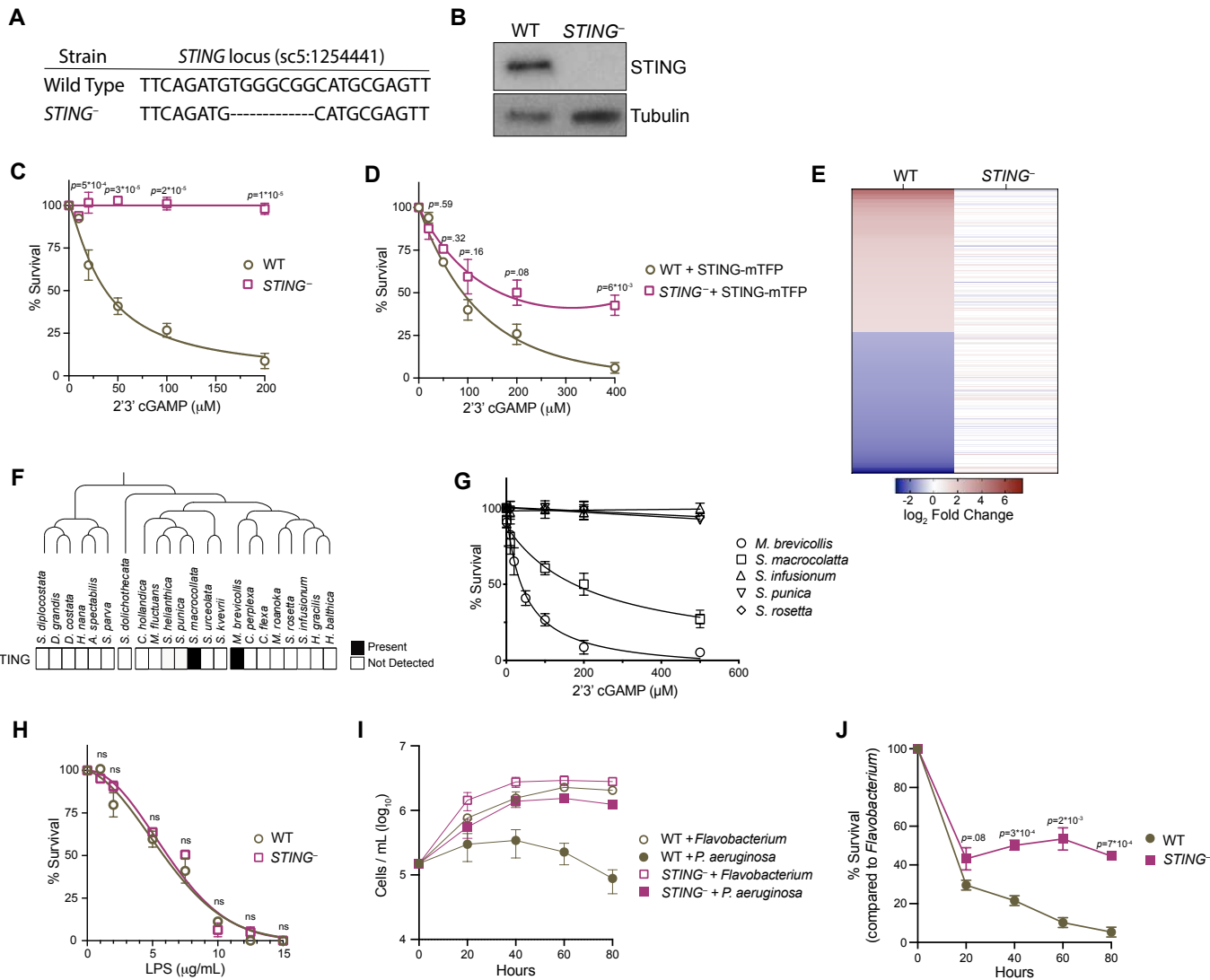
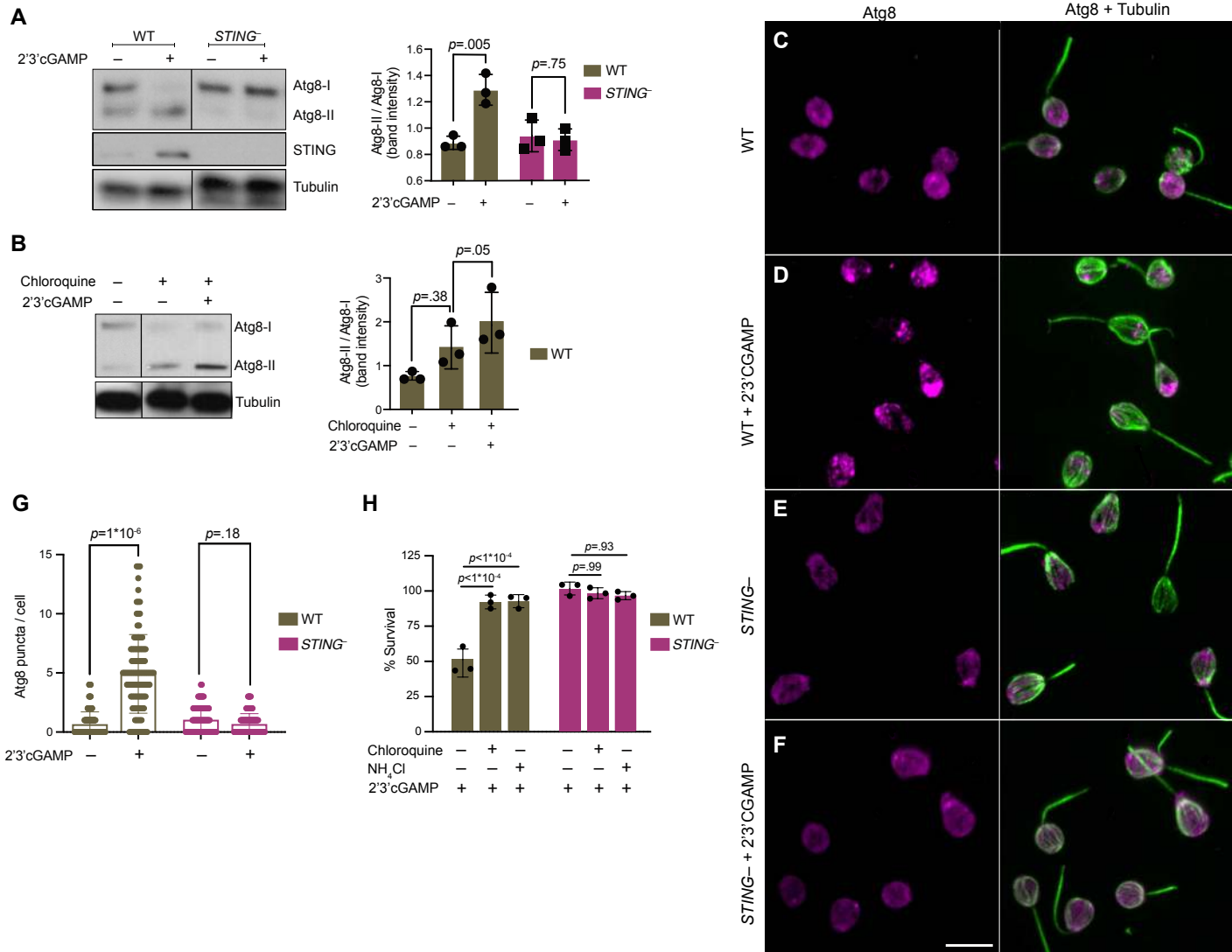


Figure 5







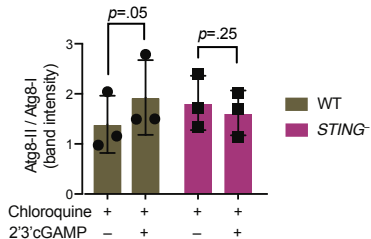
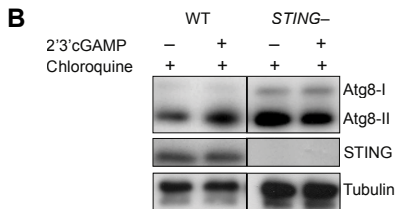
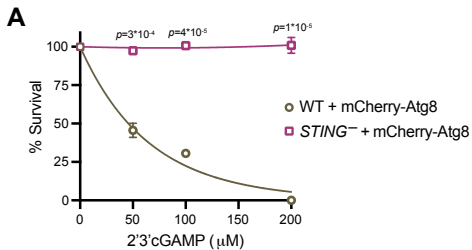


Figure 6 - figure supplement 1